Synthesis of Extractive Reaction Processes

Ketan D. Samant and Ka M. Ng
Dept. of Chemical Engineering, University of Massachusetts, Amherst, MA 01003

A systematic method presented synthesizes extractive reaction processes. The objective is to develop liquid-phase processes involving simultaneous reaction and separation by extraction to achieve improved yield, selectivity to a desired product, and separation of byproducts. The method is based on the equilibrium thermodynamic analysis of multicomponent reactive systems with multiple liquid phases. Using transformed coordinates, systems with three or fewer degrees of freedom can be conveniently analyzed regardless of the number of components in the system. Key features of the reactive phase diagrams relevant to achieving the process objectives are identified. The method is illustrated with several model examples to demonstrate the advantages of extractive reaction over conventional single-phase processes.

Introduction

In recent years, single units that combine reaction and separation operations have received considerable attention. The reduction in the number of equipment units leads to investment savings, and simultaneous reaction and separation provides the possibility of bypassing the equilibrium limitation imposed by reversible reactions. The use of reactive distillation in the production of methyl acetate and methyl *tert*-butyl ether clearly demonstrates the benefits (DeGarmo et al., 1992; Doherty and Buzad, 1992). Similar advantages have been realized with simultaneous reaction and adsorption in a chromatographic reactor (Coca et al., 1993; Tonkovich and Carr, 1994), permeation in a membrane reactor (Tsotsis et al., 1993), and extraction in a liquid–liquid two-phase reactor (Sharma, 1988). The precipitator is another type of reactive separator in which the product precipitates out of solution, thus eliminating a crystallizer from the process flow sheet (Mersmann and Kind, 1988).

In extractive reaction, a second liquid phase containing a solvent can be deliberately imposed on the system. Frequently, the solvent selectively extracts an intermediate or a product, thereby preventing its further reaction, and this results in a higher yield. For example, the epoxide product derived from 6-methylhept-5-en-2-one undergoes facile rearrangement to an undesirable by-product 1,3,3-trimethyl-2,7-dioxabicyclo[2.2.1]heptane. If the series reaction is carried out in the presence of dichloromethane, the product is extracted into the hydrocarbon phase and a higher selectivity to the epoxide product is obtained (Anderson and Veysoglu, 1973). In the Hofmann reaction of an amide with hypochlorite, a higher yield of an intermediate isocyanate can be achieved by extracting it into a selected solvent (Wang et al., 1984). Hydrolysis of formate esters with simultaneous extraction of the desired product has been shown to give superior yield and reduced waste compared to a single-phase acid hydrolysis process (King et al., 1985). In the Ruhrchemie-Rhone Poulenc process for the production of butanal by hydroformylation of propylene, the amount of heavy ends formed is reduced with a biphasic reactor (Kuntz, 1987). Not all such liquid–liquid systems are intended for reaction yield improvements. For example, Pahari and Sharma (1991) have demonstrated the removal of morpholine from dilute aqueous waste streams by reaction with benzoyl chloride dissolved in toluene. In metals processing, the recovery of a metal ion from an aqueous solution is often accomplished by reaction and extraction into an organic phase (Chapman, 1987). Since the primary objective is extraction, reactive extraction is probably a more appropriate term than extractive reaction. However, we will not make this distinction in this article.

Despite all these applications, relatively little is available on the generic issues related to the synthesis of liquid–liquid reactive systems. Specifically, it is highly desirable to understand how to exploit the reactive liquid–liquid phase behavior to generate a flow sheet for achieving different goals such as improved yield, selectivity, or ease of separations. Such an approach has been used to examine reactive distillation (Ung and Doherty, 1995a,b) and reactive crystallization systems (Berry and Ng, 1997).

Correspondence concerning this article should be addressed to K. M. Ng.

In this article we present a systematic procedure based on equilibrium thermodynamic analysis for the synthesis of extractive reaction processes. We discuss, with the aid of illustrations, the reactive phase-equilibrium calculations and the coordinate transform used to plot the reactive phase diagrams. Several examples of extractive reaction processes for improvement in yield, selectivity to a desired product, and separation of impurities are presented. These examples demonstrate the advantages of extractive reaction processes over conventional single-phase processes.

Liquid–Liquid Phase Diagrams for Systems with Reactions

In this section we present liquid–liquid phase diagrams for several hypothetical examples involving liquid–liquid phase separation and chemical reactions. We do not attempt to generate the phase diagram for any particular system. Instead, the examples considered cover several general situations. Any particular system can be analyzed similarly if relevant data are available. Some features of the reactive liquid–liquid phase diagrams will be exploited in the next section to improve yield, selectivity, or ease of separation of a process.

Generation of liquid–liquid phase diagrams for systems with reactions

The Gibbs phase rule for a reactive mixture at equilibrium can be written as

$$f = c - p - r + 2, \tag{1}$$

where f is the number of degrees of freedom, c the number of components, p the number of phases, and r the number of independent reactions. For each of the r reactions, the equilibrium constant, K_m, can be written as

$$K_m = \exp\left(\frac{-\Delta G_m}{RT}\right) \qquad m = 1, \ldots, r, \tag{2}$$

where ΔG_m is the standard Gibbs free energy of reaction, R is the gas constant, and T is the temperature. The equilibrium constant is related to species mole fractions as

$$K_m = \prod_{i=1}^{c} (x_{i,\mathrm{eq}}\gamma_{i,\mathrm{eq}})^{\upsilon_{i,m}} \qquad m = 1, \ldots, r, \tag{3}$$

where $x_{i,\mathrm{eq}}$ and $\gamma_{i,\mathrm{eq}}$ are equilibrium mole fractions and activity coefficients of component i, respectively; and $\upsilon_{i,m}$ is the stoichiometric coefficient of component i in reaction m. Stoichiometric coefficients are positive for reaction products and negative for reactants.

If the reactive system has p liquid phases at equilibrium, it also satisfies $c(p-1)$ phase equilibrium equations given by

$$\mu_j^1 = \mu_j^2 = \cdots = \mu_j^i = \cdots = \mu_j^p \qquad j = 1, 2, \ldots, c, \tag{4}$$

where μ_j^i is the chemical potential of component j in phase i. In terms of mole fractions, these equations can be written as

$$(\gamma_j x_j)^1 = (\gamma_j x_j)^2 = \cdots = (\gamma_j x_j)^i = \cdots = (\gamma_j x_j)^p \qquad j = 1, 2, \ldots, c. \tag{5}$$

In addition, for each phase i, we have:

$$\sum_{j=1}^{c} x_j = 1 \qquad i = 1, 2, \ldots, p. \tag{6}$$

The reactive phase diagrams are generated by solving Eqs. 3, 5, and 6, a total of $r + c(p-1) + p$ equations, with f variables taking specified values. We have a total of $pc + 2$ variables in this equation set; species mole fractions in each phase, temperature, and pressure.

Transformed coordinates for multicomponent phase diagrams

Representation of multicomponent phase diagrams in mole-fraction coordinates suffers from three major drawbacks. First, only diagrams with three or fewer components are easily represented. Second, reactions constrain the system to lie on a reaction-equilibrium surface that forms only a part of the composition space. Third, the lines of constant stoichiometry cannot be easily represented for all but simple reaction stoichiometries.

A coordinate system can be chosen so that all the compositions shown in a phase diagram are those on the reaction equilibrium surface. Using this transformed coordinate system also reduces the number of independent coordinates by the number of reactions without loss of any information. Phase diagrams of systems with three or fewer degrees of freedom can be easily plotted regardless of the number of components or the number of reactions.

The complete development of the coordinate transform and its application to vapor–liquid phase diagrams of reacting systems was provided by Ung and Doherty (1995a). The transform was also used by Berry and Ng (1997) for multicomponent systems with multiple solid and liquid phases and with multiple reactions in the liquid phase. Here we use the same transform for multicomponent liquid–liquid phase diagrams of reacting systems. The derivation of the transform is not provided here. However, the definition and the important properties of the $(c-r)$ transformed mole fractions, X_j $(j = 1, \ldots, c-r)$, are summarized in Appendix A. The method used for generating the reactive phase diagrams is presented in Appendix B.

Examples of Liquid–Liquid Phase Diagrams with Reactions

Three-component systems

Various types of ternary liquid–liquid phase diagrams are shown in Figure 1 (Sorenson and Arlt, 1979; Prausnitz et al., 1980). Here we consider the two most common types; type I, where only one binary pair is partially miscible, and type II, where two binary pairs are partially miscible.

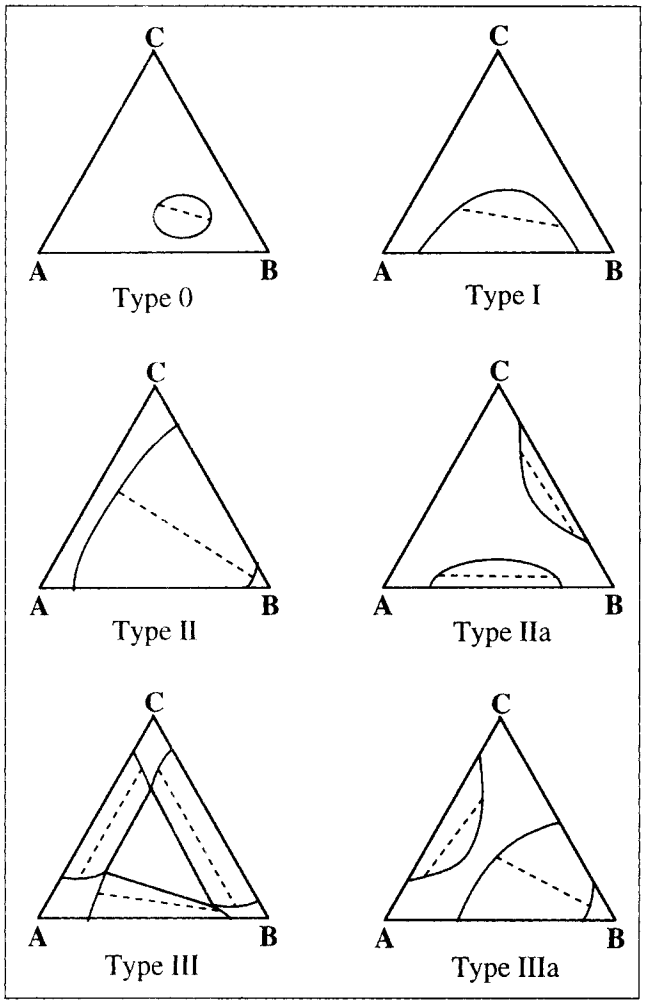

Figure 1. Types of ternary liquid–liquid equilibria.

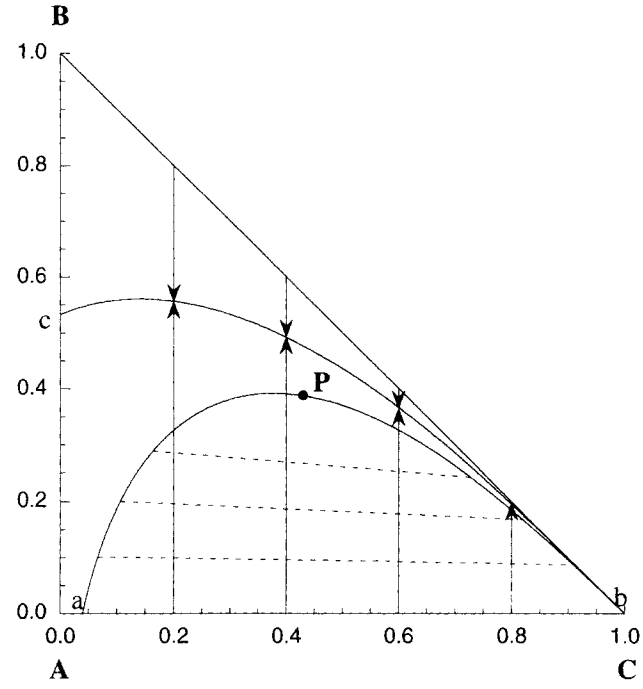

Figure 2. Phase diagram for $A \leftrightarrow B$ ($K = 1.0$) in the presence of an inert C.

Type I System with One Reaction. Consider a system that is composed of components A, B, and C with the following reaction:

$$A \leftrightarrow B, \tag{7}$$

where C is partially miscible with A. At constant temperature and pressure, Eq. 1 indicates that the system has $(2 - p)$ degrees of freedom. This means that the system has one degree of freedom and it is constrained to lie on a line in the single-phase region. In the two-phase region, it has no degrees of freedom and it is constrained to lie at a point, or more exactly, the two end points of a tie line.

Figure 2 is the phase diagram for this system with $K = 1.0$. The UNIQUAC parameters used to generate the phase diagram are listed in Table 1. Curve *aPb* is the phase envelope, point P being the plait point. Point b lies extremely close to pure-component vertex C. Curve cC is the reaction equilibrium curve. The dashes are the tie lines and the arrows are the lines of constant stoichiometry. For $K = 1.0$, the reaction equilibrium curve and the phase envelope do not intersect. Thus, the solution to Eqs. 3, 5, and 6 is the reaction equilibrium curve cC. The system is always in single phase at equilibrium. Given an initial composition, the equilibrium composition of the system corresponds to the point of intersection of the stoichiometric line through the initial composition and the curve cC.

Figure 3a is the phase diagram for the same system with $K = 0.35$. In this case, the reaction equilibrium curve cC and

Table 1. Thermodynamic Parameters Used to Generate Figures 2, 3 and 4

Figures 2 and 3		
Temperature = 298.15 K		Pressure = 1 atm
UNIQUAC Equation Parameters		
Pure-Component Parameters		
Component	r	q
A (3)	2.87	2.41
B (1)	2.204	2.072
C (2)	0.92	1.4
Binary Interaction Parameters (K)		
a (1,1) = 0.0	a (1,2) = 100.2	a (1,3) = −110.57
a (2,1) = −85.939	a (2,2) = 0.0	a (2,3) = 546.80
a (3,1) = 267.8	a (3,2) = 355.89	a (3,3) = 0.0
Figure 4		
Temperature = 307.65 K		Pressure = 1 atm
UNIQUAC Equation Parameters		
Pure-Component Parameters		
Component	r	q
A (1)	4.4998	3.856
B (2)	4.0456	3.236
C (3)	3.7165	2.816
Binary Interaction Parameters (K)		
a (1,1) = 0.0	a (1,2) = −23.434	a (1,3) = 283.89
a (2,1) = 2.2026	a (2,2) = 0.0	a (2,3) = 211.05
a (3,1) = 18.406	a (3,2) = 37.248	a (3,3) = 0.0

Source: From Sorenson and Arlt, 1979.

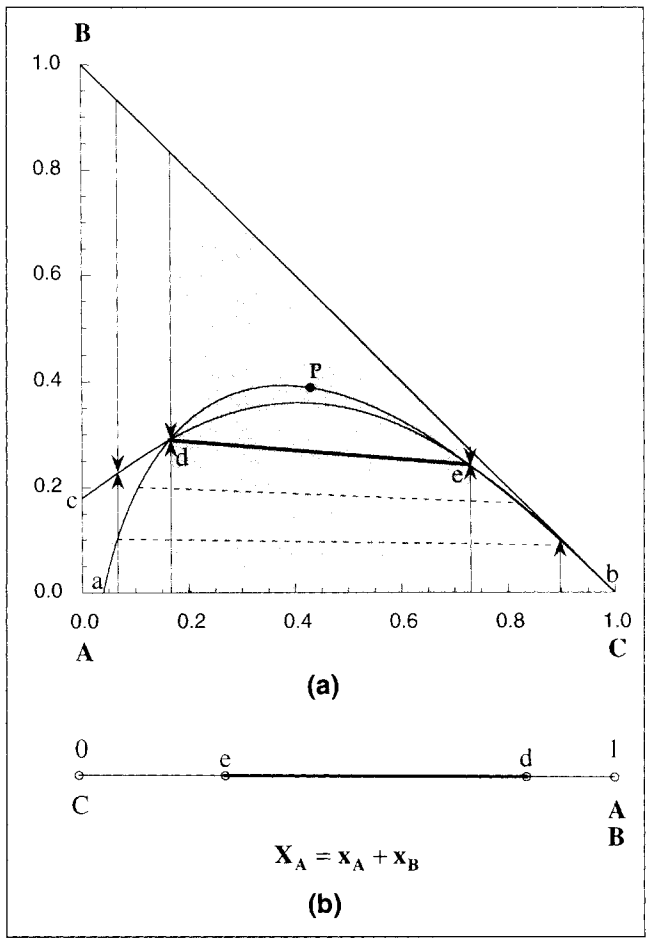

Figure 3. Phase diagrams for $A \leftrightarrow B$ ($K = 0.35$) in the presence of an inert C.

the phase envelope aPb intersect at points d and e. The shaded region bounded by the stoichiometric lines through points d and e forms the two-phase region of the phase diagram. If the initial composition of the system lies in this region, at equilibrium the system would split into two phases with compositions corresponding to points d and e. Line de is the unique reactive tie line for the system. Outside the shaded region, the system is always in single phase and the equilibrium compositions lie on sections cd and eC of the curve cC.

The phase diagram for this system can also be plotted in the transformed coordinates. Using B as the reference component, the transformed coordinates are

$$X_A = x_A + x_B \tag{8}$$

$$X_C = x_C. \tag{9}$$

Since only one of these coordinates is independent, the phase diagram is a line as shown in Figure 3b. The point $X_A = 0$ corresponds to pure component C and the point $X_A = 1$ corresponds to either pure component A, pure component B, or the equilibrium mixture of A and B. The end points d and e of the reactive tie line bound the two-phase region. Any initial composition within this region would give rise to two phases with compositions corresponding to points d and e. The relative amounts of the two phases can be calculated using the lever rule in terms of transformed coordinates as shown in Appendix C.

Type II System with One Reaction. Consider a system of components A, B, and C with the following reaction:

$$A + B \leftrightarrow C, \tag{10}$$

where C is partially miscible with both A and B. The UNIQUAC parameters for this system are also listed in Table 1. This system also has one degree of freedom in the single-phase region and no degrees of freedom in the two-phase region at constant temperature and pressure.

Figure 4a is the phase diagram for this system with $K = 10.0$. Curves ab and cd are the phase-equilibrium curves and curve $BefhgA$ is the reaction-equilibrium curve. The dashes are the tie lines and the arrows the stoichiometric lines. Points e, f, h, and g are the points of intersection of the phase and reaction equilibrium curves. Thus, we have two reactive tie lines ef and gh. Stoichiometric lines through the end points of these tie lines form two separate two-phase regions (shaded) for this system. Within these regions, the system splits into two phases corresponding to the end points of the reactive tie line in that region. Outside these regions, the sys-

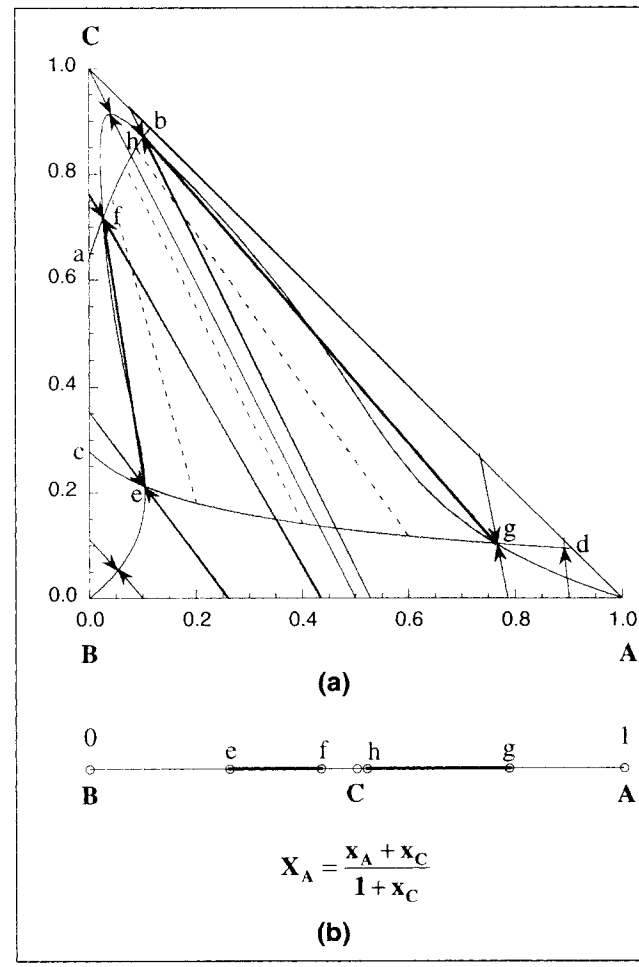

Figure 4. Phase diagrams for $A + B \leftrightarrow C$ ($K = 10.0$).

tem is in single phase and the equilibrium compositions would lie on sections *Be*, *fh*, or *gA* of the equilibrium curve.

Using *C* as the reference component, the transformed coordinates are

$$X_A = \frac{x_A + x_C}{1 + x_C} \tag{11}$$

$$X_B = \frac{x_B + x_C}{1 + x_C}. \tag{12}$$

The phase diagram in these coordinates is shown in Figure 4b. Point $X_A = 0$ corresponds to pure *B*, point $X_A = 1$ corresponds to pure *A*, and point $X_A = 0.5$ corresponds to pure *C* as well as to the equilibrium mixture of *A*, *B*, and *C*. Regions *ef* and *gh* are the two two-phase regions. Any initial composition within each of these regions would give rise to two phases with compositions corresponding to the end points of that region. Again, the lever rule in terms of transformed coordinates should be used for this phase diagram for determining the relative amounts of each phase.

Four-component systems

Figure 5 shows various types of quaternary liquid–liquid phase diagrams (Sorenson and Arlt, 1979; Prausnitz et al., 1980). Here we consider the three most common types: type I, type II, and type III, with one, two, and three partially miscible pairs, respectively.

Four Component Systems with One Reaction. Consider a quaternary system of components *A*, *B*, *C*, and *D* with the reaction

$$B + C \leftrightarrow D. \tag{13}$$

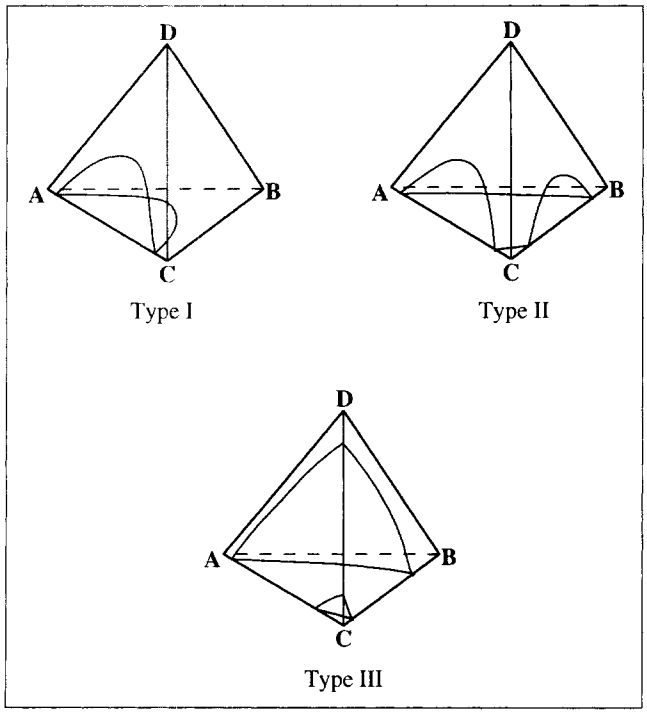

Figure 5. Types of quaternary liquid–liquid equilibria.

Table 2. Thermodynamic Parameters for Four Component Systems

Temperature = 298.15 K		Pressure = 1 atm	
UNIQUAC Equation Parameters			
Pure-Component Parameters for Type I System (Figure 6)			
Component		r	q
A (1)		2.2024	2.072
B (2)		3.4543	3.052
C (3)		3.1878	2.400
D (4)		2.4088	2.248
Binary Interaction Parameters (K) for Type I System			
$a(1,1)=0.0$	$a(1,2)=-277.29$	$a(1,3)=56.488$	$a(1,4)=-229.71$
$a(2,1)=157.60$	$a(2,2)=0.0$	$a(2,3)=17.119$	$a(2,4)=-25.154$
$a(3,1)=41.146$	$a(3,2)=154.55$	$a(3,3)=0.0$	$a(3,4)=649.05$
$a(4,1)=121.11$	$a(4,2)=7.4068$	$a(4,3)=113.53$	$a(4,4)=0.0$
Pure-Component Parameters for Type II System (Figure 7)			
Component		r	q
A (1)		4.0464	3.240
B (2)		2.8768	2.612
C (3)		3.9228	2.968
D (4)		0.9200	1.400
Binary Interaction Parameters (K) for Type II System			
$a(1,1)=0.0$	$a(1,2)=241.71$	$a(1,3)=-127.86$	$a(1,4)=1247.3$
$a(2,1)=-89.784$	$a(2,2)=0.0$	$a(2,3)=-160.03$	$a(2,4)=295.53$
$a(3,1)=187.68$	$a(3,2)=165.64$	$a(3,3)=0.0$	$a(3,4)=950.60$
$a(4,1)=540.36$	$a(4,2)=-140.02$	$a(4,3)=350.21$	$a(4,4)=0.0$
Pure Component Parameters for Type III System (Figure 8)			
Component		r	q
A (1)		3.9228	2.968
B (2)		5.1742	4.396
C (3)		2.5445	2.264
D (4)		8.3279	7.600
Binary Interaction Parameters (K) for Type III System			
$a(1,1)=0.0$	$a(1,2)=167.10$	$a(1,3)=43.639$	$a(1,4)=30.143$
$a(2,1)=-70.699$	$a(2,2)=0.0$	$a(2,3)=111.39$	$a(2,4)=14.554$
$a(3,1)=46.479$	$a(3,2)=102.49$	$a(3,3)=0.0$	$a(3,4)=17.522$
$a(4,1)=231.75$	$a(4,2)=130.11$	$a(4,3)=581.46$	$a(4,4)=0.0$

Source: From Sorenson and Arlt, 1979.

We consider *D* to be partially miscible with *C* for a type I system, partially miscible with *A* and *C* for a type II system, and partially miscible with *A*, *B*, and *C* for a type III system. The UNIQUAC parameters used for each of these systems are listed in Table 2.

The isobaric, isothermal phase diagram for a quaternary system can be plotted as a regular tetrahedron in mole-fraction coordinates. The solutions to the reaction-equilibrium equations, Eqs. 3 and 6, and the phase-equilibrium equations, Eqs. 5 and 6, will lie on surfaces within this tetrahedron. If the reaction and phase equilibrium surfaces do not intersect, the system will always be in single phase and the equilibrium composition of the system will lie on the reaction-equilibrium surface. If the two surfaces intersect, the region of intersection gives the compositions where the system splits into two phases at equilibrium. Since the system has $4(c) - 2(p) - 1(r) = 1$ degree of freedom under these conditions, this region is a curve. In the rest of the composition space, the system will be in single phase with compositions lying on the reaction-equilibrium surface.

Plotting the phase- and reaction-equilibrium surfaces and identifying the compositions that satisfy both phase and reaction equilibrium is difficult using mole-fraction coordinates. We can considerably simplify the task by using the transformed coordinates. Using D as a reference component, the transformed coordinates are

$$X_A = \frac{x_A}{1 + x_D} \tag{14}$$

$$X_B = \frac{x_B + x_D}{1 + x_D} \tag{15}$$

$$X_C = \frac{x_C + x_D}{1 + x_D}. \tag{16}$$

The phase diagram can be plotted in two dimensions, as only two of these coordinates are independent.

Figure 6a shows the curve (curve *apb*) of intersection of the phase and the reaction equilibrium surfaces for the type I system. The dashed lines are tie lines. Points a and b lie on the BCD surface, whereas point p lies within the tetrahedron. For this system, the phase diagram in terms of transformed coordinates X_A and X_B is shown in Figure 6b. The vertices correspond to pure components A, B, and C as marked in the figure. The point $X_A = 0$, $X_B = 0.5$ corresponds to pure D as well as to an equilibrium mixture of B, C, and D. The region bounded by line ab and the curve apb represents the two-phase region. Reactive tie lines within this region are shown as dashed lines. Any initial composition within this region would split into two phases with compositions corresponding to the end points of tie lines passing through it. The relative amounts of each phase can be determined using the lever rule in transformed coordinates. It should be noted that the plait point p of the reactive phase diagram does not necessarily correspond to the plait point of the phase-equilibrium surface, which is not shown here.

Figures 7a and 7b are similar plots for the type II system. Again, the region *apba* on Figure 7b represents the two-phase region. Figures 8a and 8b are similar plots for the type III system. In this case D is partially miscible with the rest of the components. The intersection of the phase- and the reaction-equilibrium surfaces is in the form of two curves, *ab* and *cd*, connected by tie lines as shown in Figure 8a. Points a, b, c, and d all lie on the BCD surface. The two-phase region on the transformed coordinate diagram takes the form of a bandlike region bounded by curves *ac* and *bd*. This type of phase behavior can be utilized effectively for separation of hard-to-separate impurities from product streams.

Synthesis of Reactive Extraction Processes

In many processes, extractive reaction can be used as a useful alternative for improvement in yield of a desired prod-

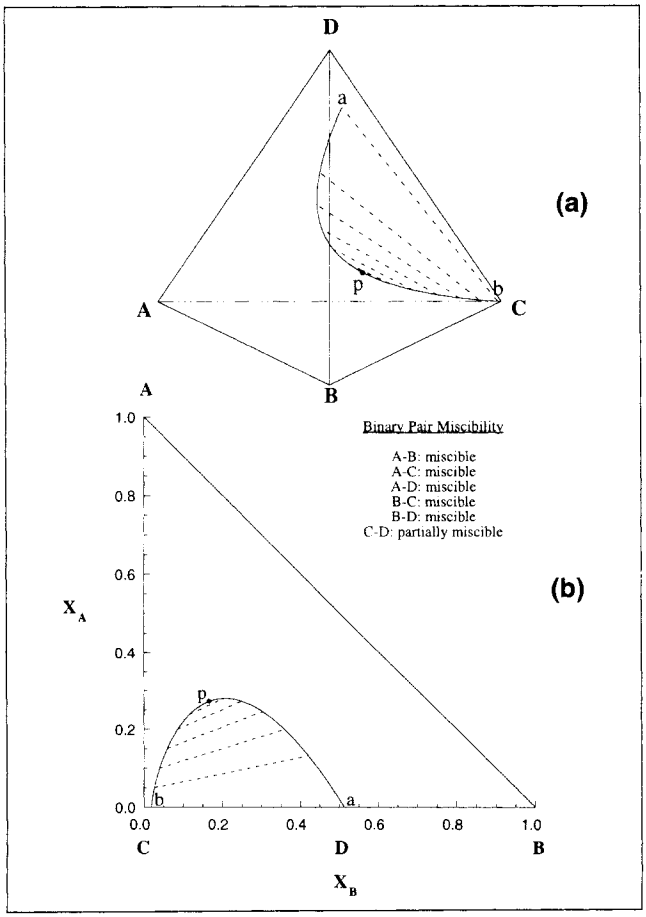

Figure 6. Phase diagrams for $B + C \leftrightarrow D$ with an inert A: type I system.

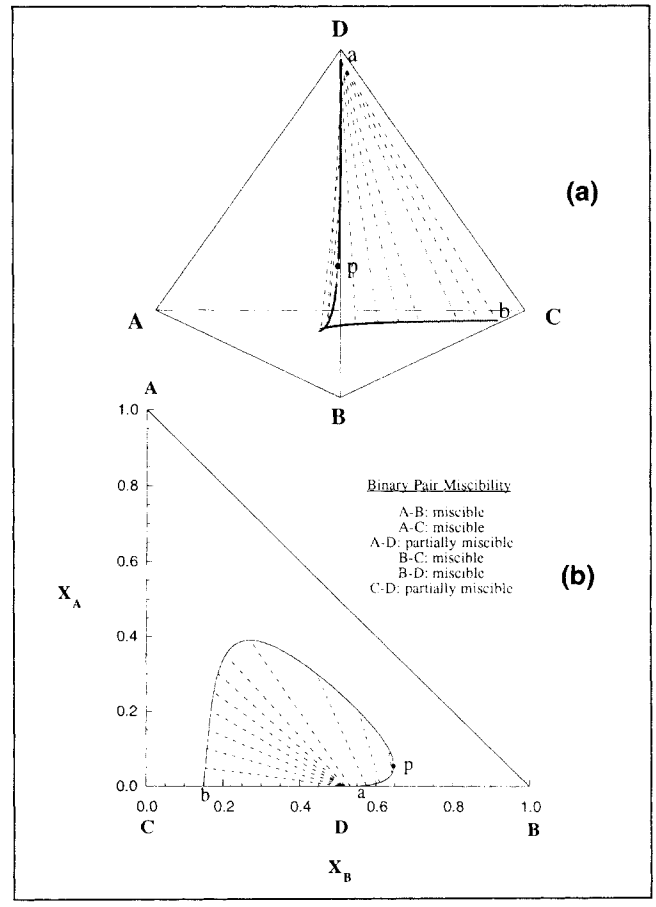

Figure 7. Phase diagrams for $B + C \leftrightarrow D$ with an inert A: type II system.

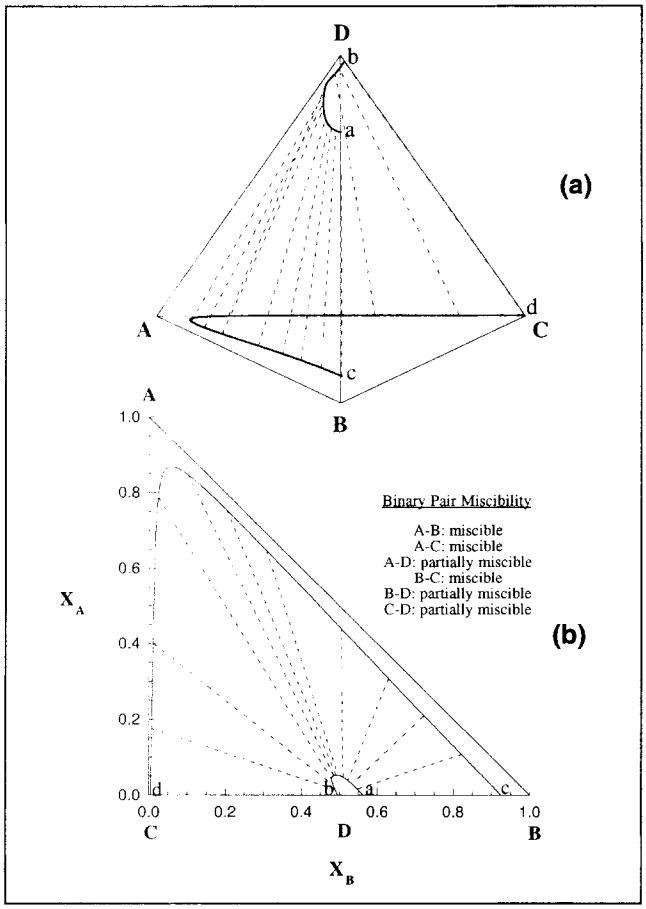

Figure 8. Phase diagrams for $B + C \leftrightarrow D$ with an inert A: type III system.

uct, selectivity to a desired product, and ease of separation. In this section, we demonstrate the use of the reactive phase diagrams for synthesizing extractive reaction processes that meet these objectives. The examples presented are based on realistic thermodynamic parameters.

Processes for Improvement in Yield

Reactive extraction processes can be synthesized for improving the yield of a desired product, defined as

$$\text{Yield} = \frac{\text{Amount of desired product produced}}{\text{Amount of reactant fed to the reactor}}, \quad (17)$$

in many reactive systems. The yield as defined here is the per-pass yield. The overall yield from both the single-phase and the extractive-reaction processes will always be 100% if all the unconverted reactants are recycled without any loss. Low per-pass yield from a single-phase process implies large loads on the separation system and large recycle flows. Using an extractive reaction we increase the per-pass yield considerably, thus decreasing the recycle of unconverted reactants. But extractive reaction processes also involve recovery and recycle of an inert solvent. However, a judicious choice of solvent can keep this recycle flow low. Improvement in per-pass yield becomes especially significant when reactants are lost through purge or waste streams, as is usually the case with many industrial processes.

Example I: Use of Solvent to Extract the Desired Product. Yield of the desired product can be substantially improved by employing a solvent that is completely miscible with it and partially miscible with other reactants and products. In this case, extraction of the desired product into the solvent-rich phase pushes the reaction equilibrium to the right, thus increasing the yield.

Consider a system with reaction:

$$A \leftrightarrow B. \quad (18)$$

Solvent I is completely miscible with B but partially miscible with A. Figure 9 shows the phase diagram in mole-fraction coordinates for this system. The solid line passing through plait point P is the phase envelope and the dotted line through points E and R is the reaction equilibrium curve. The shaded region represents the two-phase region in the presence of the reaction. It is bounded by the horizontal stoichiometric lines through points E and R. Any feed composition within this region would split into two phases with compositions corresponding to points E and R. The solvent-rich phase is termed as the extract (E) and the solvent-lean phase as the raffinate (R).

Point (e) represents the reactor effluent composition if we operate the system without adding solvent I. If we choose solvent I such that A and I are highly immiscible and the tie lines slope toward A, the extract (E) is much richer in B than point (e). We can take advantage of this feature to design a process for improving the yield of B.

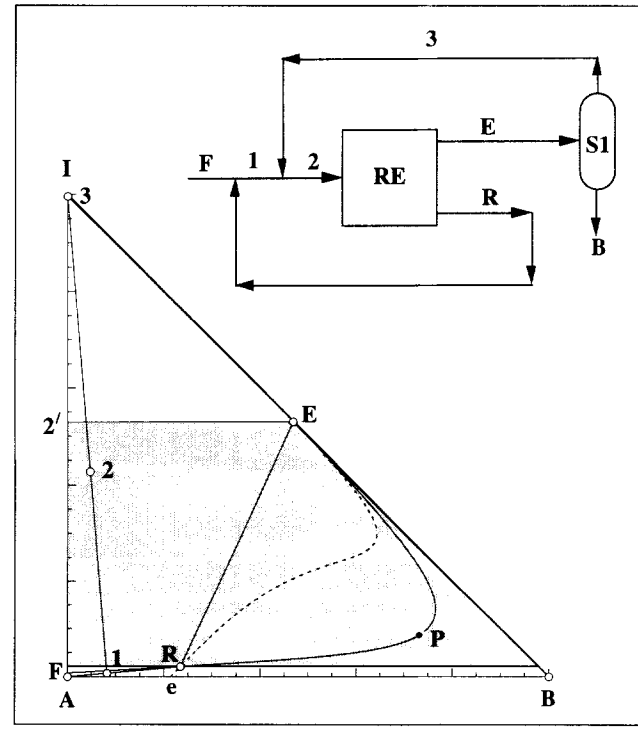

Figure 9. Improvement in yield: flowsheet and phase diagram for Example I.

Table 3. Degrees of Freedom for Examples I to V

	Examples			
	I and II	III	IV	V
No of components (c)	3	4	5	5
No. of reactions (r)	1	1	2	2
No. of stages	1	N	N	N
No. of streams (s)	7	$2N+9$	$2N+11$	$2N+9$
No. of variables	28	$10N+46$	$12N+67$	$12N+55$
No. of equations	21	$10N+28$	$12N+40$	$12N+33$
Deg. of freedom	7	18	27	22
Variables specified	Flow rate of (B)	Flow rate of (B)	Flow rate of (B)	Flow rate of (B)
	Composition of (B)	Compositions of (A), (B), (C), and (I)	Compositions of (A), (B), (C), (D), and (I)	Compositions of (A), (B), (C), and (I)
	Composition of (F)			
	Mole fraction of B in (3)	Mole fraction of I in (2)	Mole fraction of D in (2)	Mole fraction of I in (2)
		Mole fraction of C in (3)	Mole fraction of I in (3)	Mole fraction of C in (3)
		Mole fraction of B in (1)	Mole fraction of C in (4)	Mole fraction of B in (1)
		Mole fraction of B in (R)	Mole fraction of B in (1)	Mole fraction of B in (R)
			Mole fraction of B in (R)	
Design Variable	Flow rate of (R)	Mole fraction of B in (E)	Mole fraction of B in (E)	Mole fraction of B in (E)

Figure 9 also shows a flow sheet for such a process. Stream numbers on the flow sheet and the points on the phase diagram correspond to one another. The feed (F, pure A) is combined with the raffinate (R) from the reactor RE and recycle stream (3) from the separator $S1$ to make stream (2). This stream forms the feed to the reactor. As (2) lies within the shaded region, the reactor effluent comprises the extract (E) and the raffinate (R) streams. The raffinate is recycled and the extract is sent to $S1$ where pure B is separated. Conceptually, this flow sheet is similar to the continuously stirred decanting reactor discussed by Harold et al. (1996).

The degrees-of-freedom analysis for the flow sheet is summarized in Table 3. Three degrees of freedom are specified by fixing the composition and production rate of stream (B), two by fixing composition of feed (F), and one by specifying complete separation of B in $S1$; that is, no B in stream (3). The remaining degree of freedom can be specified by fixing flow rate of raffinate (R).

The yield from the process is influenced by the choice of raffinate flow rate. Figure 10 shows percentage yield of B as a function of raffinate flow rate. Feed composition (point 2) approaches point 2′ as R tends to zero. As R decreases toward zero, the amounts of A and B being recycled through the raffinate stream decrease and tend to zero. Thus the yield of B tends to a maximum value that depends on the equilibrium phase behavior of the system (location of point E). For this example, as E lies extremely close to the $I-B$ edge, A in the feed stream is almost completely consumed. However, as R decreases, the solvent flow rate increases. The operation at vanishingly low values of R is not practical due to the prohibitively high amounts of solvent needed and due to the kinetic and transport limitations. In some cases, high yield can also be obtained by operating in the single-phase region above the line $2'E$. However, prohibitively high amounts of solvent I may be needed to operate in this region. Thus this option may not offer any significant advantage.

Example II: Use of Solvent Miscible with Reactants and Products. When phase separation already exists in the reaction mixture, yield of a desired product can be improved by the addition of a solvent completely miscible with the reactants and products. Consider the following system where B is the desired product:

$$A \leftrightarrow B. \tag{19}$$

Reactant A and product B are partially miscible. Hence at fixed temperature and pressure the system has $2(c)-1(r)-p=(1-p)$ degrees of freedom. Thus at equilibrium the system will always be in single phase. Figure 11a shows the phase diagram for this two-component system. Equilibrium compositions would lie on sections Aa and bB, depending on the value of the equilibrium constant K. The two-phase region ab is infeasible. If we are constrained to operate at a fixed temperature and pressure and if the value of K under these constraints is such that the equilibrium composition lies in the region Aa, the yield of B is very poor. For improvement in yield, it is desirable to cross over to the other side of the two-phase region. This can be done by adding solvent I miscible with both A and B, thus providing the system with one more degree of freedom at constant temperature and pressure.

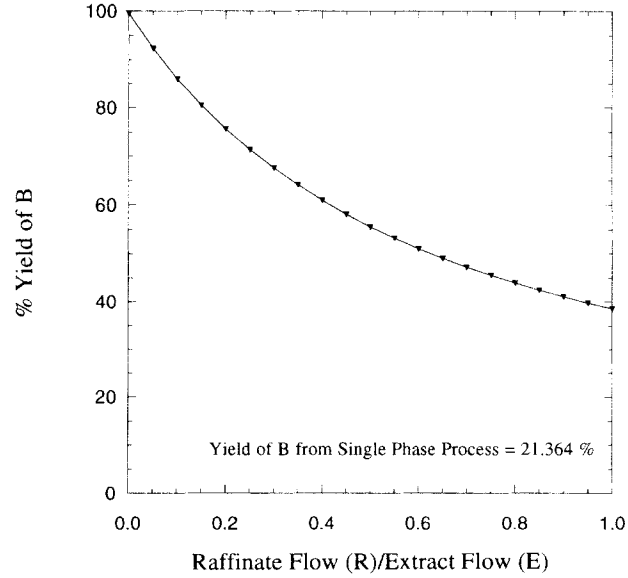

Figure 10. Yield of B as a function of raffinate flow rate for Example I.

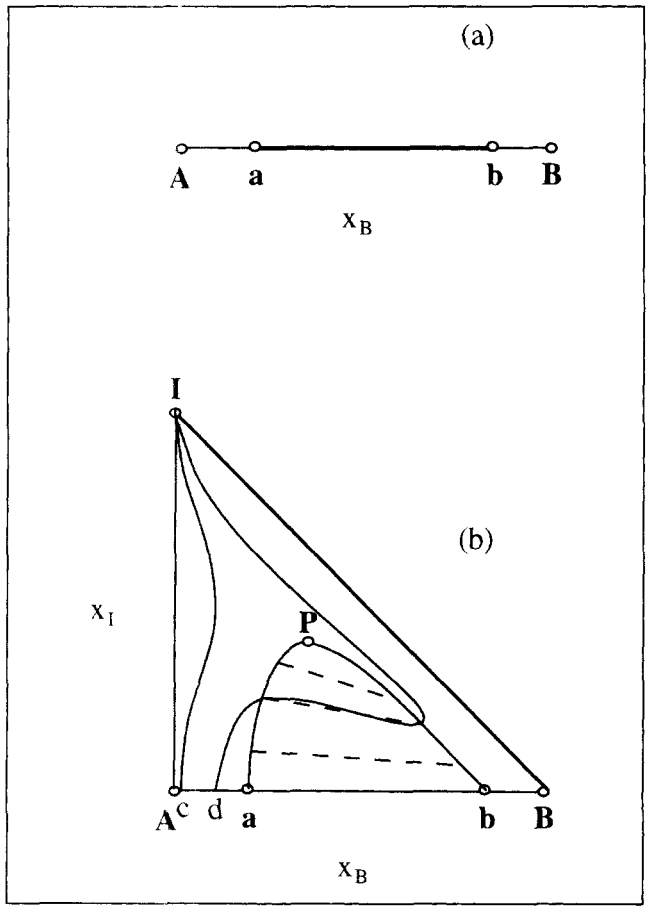

Figure 11. Use of solvent miscible with reactants and products for improvement in yield.

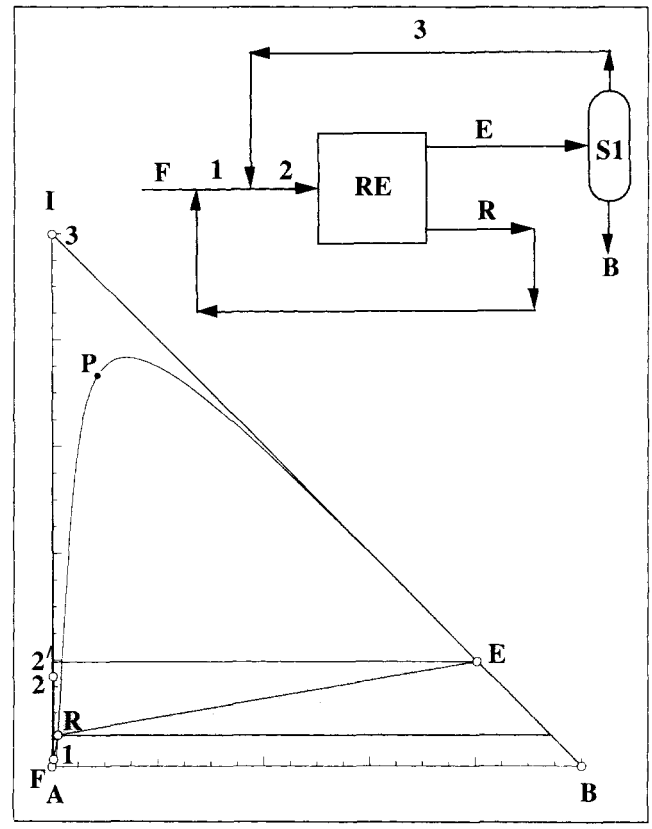

Figure 12. Improvement in yield: flowsheet and phase diagram for Example II.

Figure 11b shows the phase envelope *aPb* for the three-component system. Each point on the branch *aP* is connected to a point on branch *Pb* by a tie line, and this pair has a value of K associated with it. We can cross over to the other side of the phase envelope if the reaction equilibrium curve starting at any point along *Aa* intersects the branch *aP*. This will happen if and only if K corresponding to this point lies within the range spanned by K values on *aP*. Care should be taken in choosing a solvent to ensure that this indeed is the case. This is illustrated in Figure 11b, which shows the reaction equilibrium curves starting from points *c* and *d* corresponding to different values of K. The value of K at point *c* does not lie within the range of K values on *aP*, while the value of K at point *d* lies within this range. Hence, addition of solvent *I* is not useful when the equilibrium composition of the single-phase system corresponds to point *c*, but is useful when the equilibrium composition of the single-phase system corresponds to point *d*.

A typical phase diagram is shown in Figure 12. The solid line passing through plait point *P* is the phase envelope and line *RE* is the reactive tie line. The shaded region bounded by stoichiometric lines through *E* and *R* forms the two-phase region. The flow sheet used for the previous process can also be used here, as shown in Figure 12.

As before the raffinate (R) flow rate has to be specified as a degree of freedom. The improvement in yield as a function of raffinate flow is shown in Figure 13. In this case, too, the yield of *B* tends to a theoretical maximum as R decreases and tends to zero. For the thermodynamic parameters chosen for this example, this maximum is close to 100%. The increase in yield with decreasing R should be traded off

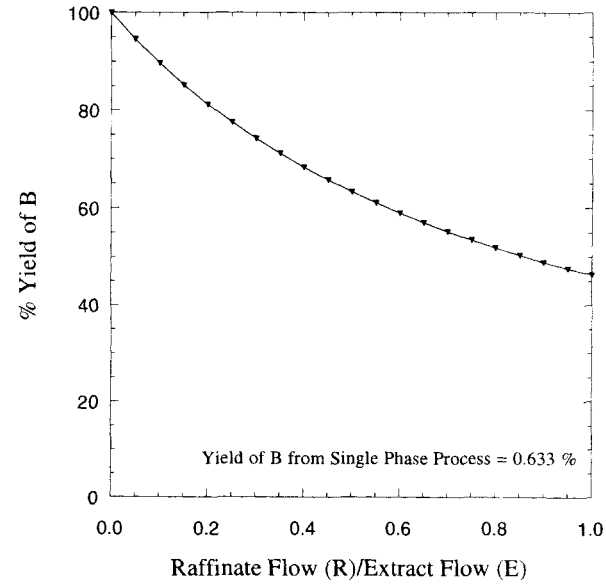

Figure 13. Yield of *B* as a function of raffinate flow rate for Example II.

against the increase in solvent flow with a decrease in R. Compared to less than 1% yield in the single-phase process, the improvement in yield at all values of R is very significant.

Example III: Use of Solvent Partially Miscible with the Desired Product. For multiproduct reactions, the yield of the desired product can be increased by using a solvent partially miscible with it and completely miscible with other reactants and products. For example, consider a reaction:

$$A \leftrightarrow B + C. \tag{20}$$

Solvent I is completely miscible with A and C, but partially miscible with the desired product B. Using A as the reference component, the transformed coordinates for this system are

$$X_B = \frac{x_B + x_A}{1 + x_A} \tag{21}$$

$$X_C = \frac{x_C + x_A}{1 + x_A} \tag{22}$$

$$X_I = \frac{x_I}{1 + x_A}. \tag{23}$$

Figure 14 shows the phase diagram for this system in transformed coordinates. At constant temperature and pressure, the system has $4(c) - 1(r) - 2(p) = 1$ degree of freedom in the two-phase region and $4(c) - 1(r) - 1(p) = 2$ degrees of freedom in the single-phase region. Each region has one more degree of freedom than the previous examples. Thus we can use a countercurrent multistage extractive reaction (MSER) process for this system. The countercurrent MSER cascade is shown in the inset of Figure 14. All stages in the cascade are theoretical stages. The liquid phases leaving each stage are perfectly mixed and are in phase and reaction equilibrium. Thus their compositions lie on the phase envelope in the transformed coordinate diagram.

Flowsheet for the MSER process is also shown in Figure 14. The stream numbers on the flowsheet correspond to the points marked on the phase diagram. Pure B is separated from the raffinate stream (R) in separator $S1$. Stream (1) from $S1$ is mixed with I obtained from separator $S2$ to form the solvent stream (S). The extract (E), rich in I, is fed to separator $S2$ where I is separated. C is removed from stream (2) of $S2$ in separator $S3$. Stream (3) from $S3$ is mixed with fresh reactant A to form the feed (F) to the MSER cascade.

Reaction occurs only in the MSER cascade and not in the separators $S1$, $S2$, and $S3$. Hence, the material balance lines joining the feed and effluent streams of the MSER cascade obey the lever rule in terms of transformed coordinates. However, as shown in Appendix C, although the material balance lines for the rest of the flow sheet obey the lever rule in terms of transformed coordinates, they are constrained by additional equations. It is for this reason that in the phase diagram of Figure 14 and in the diagrams to follow, the feed and effluent streams from MSER cascade are shown by filled circles and all other streams by open circles.

The degrees-of-freedom analysis for this process is summarized in Table 3. Mole fraction of B in the raffinate phase, $x_{B,R}$ (or equivalently $X_{B,R}$), is fixed and mole fraction of B in

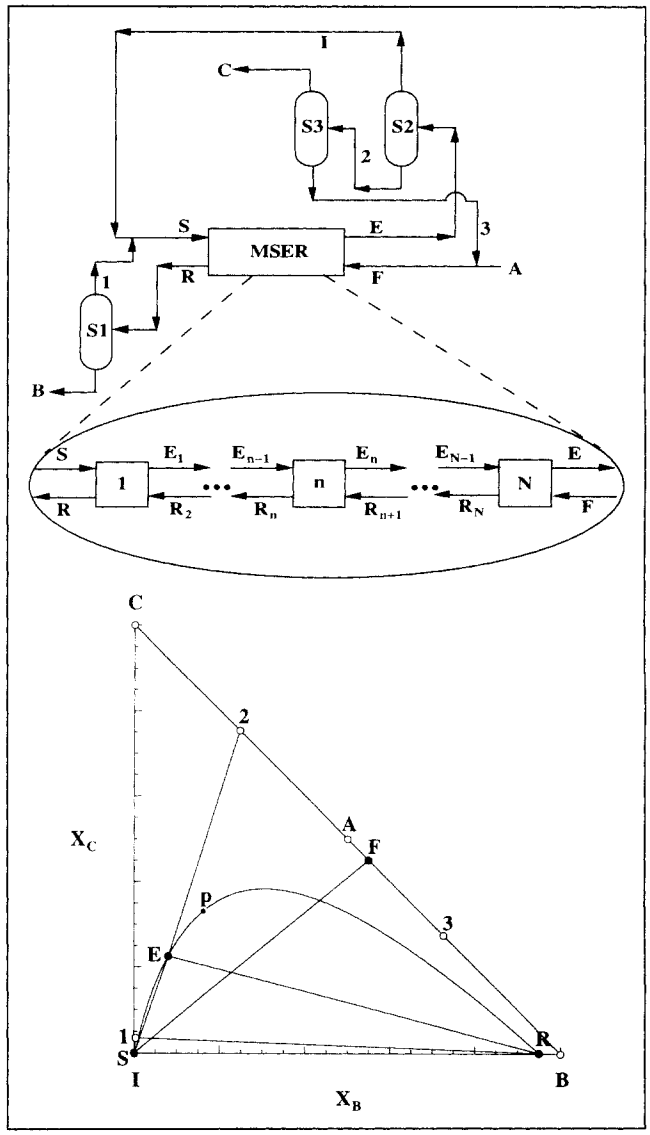

Figure 14. Improvement in yield: flowsheet and phase diagram for Example III.

the extract phase, $x_{B,E}$ (or equivalently $X_{B,E}$), is chosen as the design variable. Figure 15a shows the percentage yield of B from the process as a function of $X_{B,E}$. The yield goes through a maximum as point E moves toward the plait point p of the reactive phase envelope. For any chosen $X_{B,E}$, the yield from the process is better than its single-phase counterpart; that is, I is not added. Figure 15b shows the effect of $X_{B,E}$ on flow rates of the feed and effluent streams to the cascade and on the number of theoretical stages needed. As expected, a trade-off is observed between the flows and the theoretical stage requirement. For low values of $X_{B,E}$, a small number of stages are required, but the flows increase very sharply. For higher values of $X_{B,E}$, the flows are smaller, but the stage requirement increases sharply.

Processes for Improvement in Selectivity

In systems with multiple reactions, extractive reaction can be used to improve the selectivity to a desired product. The

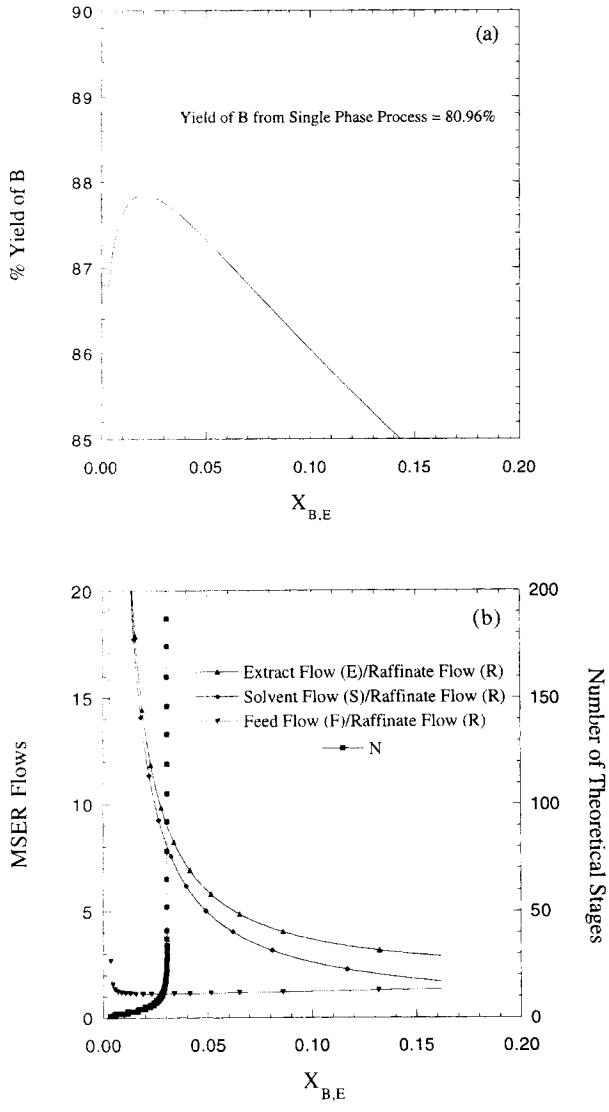

Figure 15. (a) Yield of *B* as a function of extract composition for Example III; (b) trade-off between process flows and stage requirement for Example III.

selectivity to the desired product is parametrized by the product distribution as

$$\text{Product distribution} = \frac{\text{Amount of desired product produced}}{\text{Amount of reactant consumed}}. \tag{24}$$

Example IV: Series or Parallel Reactions. Consider a system with reactions in parallel:

$$A \leftrightarrow B + C \tag{25}$$
$$A \leftrightarrow D,$$

or with reactions in series:

$$A \leftrightarrow B + C \leftrightarrow D. \tag{26}$$

As we are concerned with the equilibrium analysis only, Eqs. 25 and 26 are equivalent. Both the reaction schemes can be represented by either of the two equations. However, it should be noted that Eqs. 25 and 26 are not equivalent when we consider the effect of reaction kinetics and transport on the equilibrium analysis. In both cases, the selectivity to the desired product *B* is parametrized by the product distribution as

$$\text{Product distribution} = \frac{\text{Total } B \text{ produced}}{\text{Total } A \text{ reacted}}. \tag{27}$$

Solvent *I*, completely miscible with components *A*, *C*, and *D* but partially miscible with *B*, can be used. The phase diagram for this five-component system is shown in Figure 16.

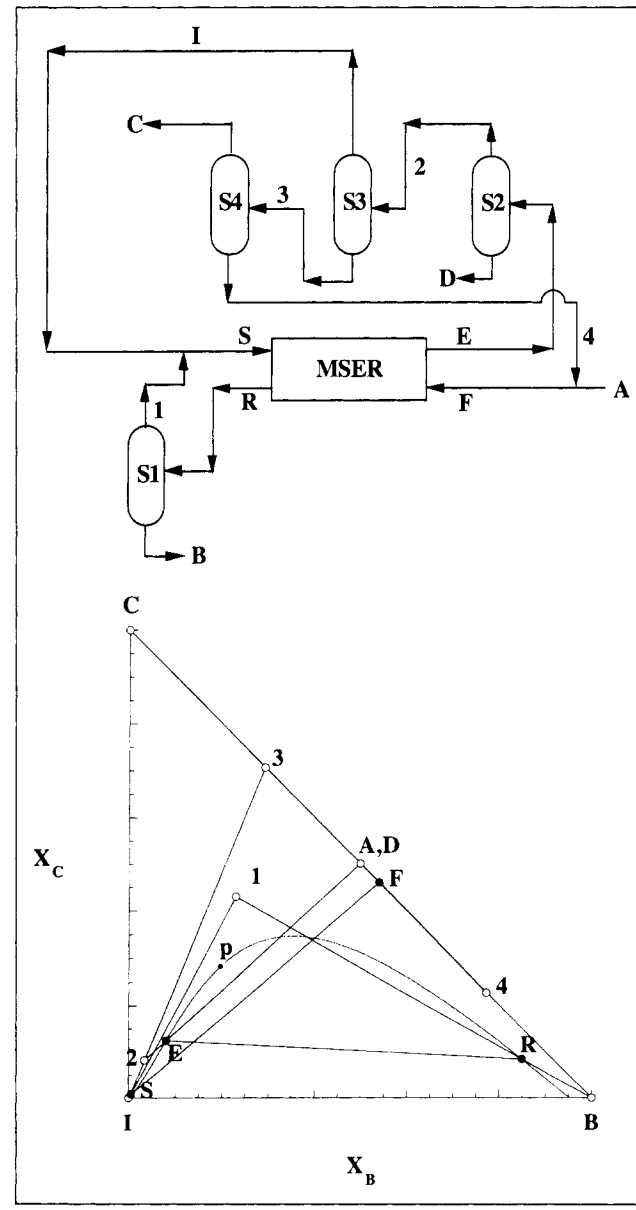

Figure 16. Improvement in selectivity: series and parallel reactions: flowsheet and phase diagram for Example IV.

With A and D as the reference components, the transformed coordinates are

$$X_B = \frac{x_B + x_A + x_D}{1 + x_A + x_D} \tag{28}$$

$$X_C = \frac{x_C + x_A + x_D}{1 + x_A + x_D} \tag{29}$$

$$X_I = \frac{x_I}{1 + x_A + x_D}. \tag{30}$$

The system, at constant temperature and pressure, has $5(c) - 2(r) - 2(p) = 1$ degree of freedom in the two-phase region and $5(c) - 2(r) - 1(p) = 2$ degrees of freedom in the single-phase region. Thus as shown in the flow sheet in Figure 16, the countercurrent MSER cascade can be used for this system. The streams in the flow sheet are identified by open and filled circles on the phase diagram. The flow sheet is similar to the one used in the previous example except the separation sequence for the extract stream (E). D is separated from the extract (E) in separator $S2$. Stream (2) from $S2$ is sent to separator $S3$ where I is removed and then combined with stream (1) to make the solvent stream (S). Separator $S4$ removes product C from stream (3). Stream (4) is combined with reactant A to form the feed (F).

The degrees-of-freedom analysis for this flowsheet is similar to Example III (Table 3). The composition of B in the extract phase ($x_{B,E}$ or $X_{B,E}$) is chosen as the design variable. As shown in Figure 17, the product distribution becomes more and more favorable as $X_{B,E}$ increases toward the plait point p. For all values of $X_{B,E}$, the product distribution is superior to that obtained from a single-phase process. It should be noted that a trade-off in the stream flows to the MSER cascade, and the theoretical stage requirement, similar to the previous example, is also observed in this case.

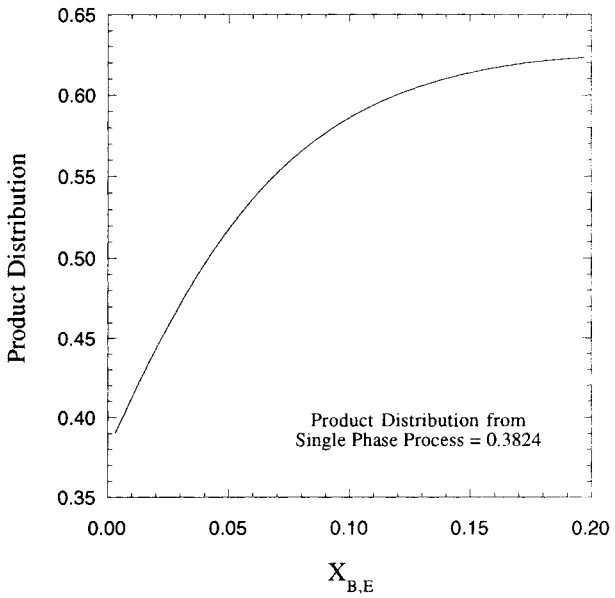

Figure 17. Product distribution as a function of extract composition for Example IV.

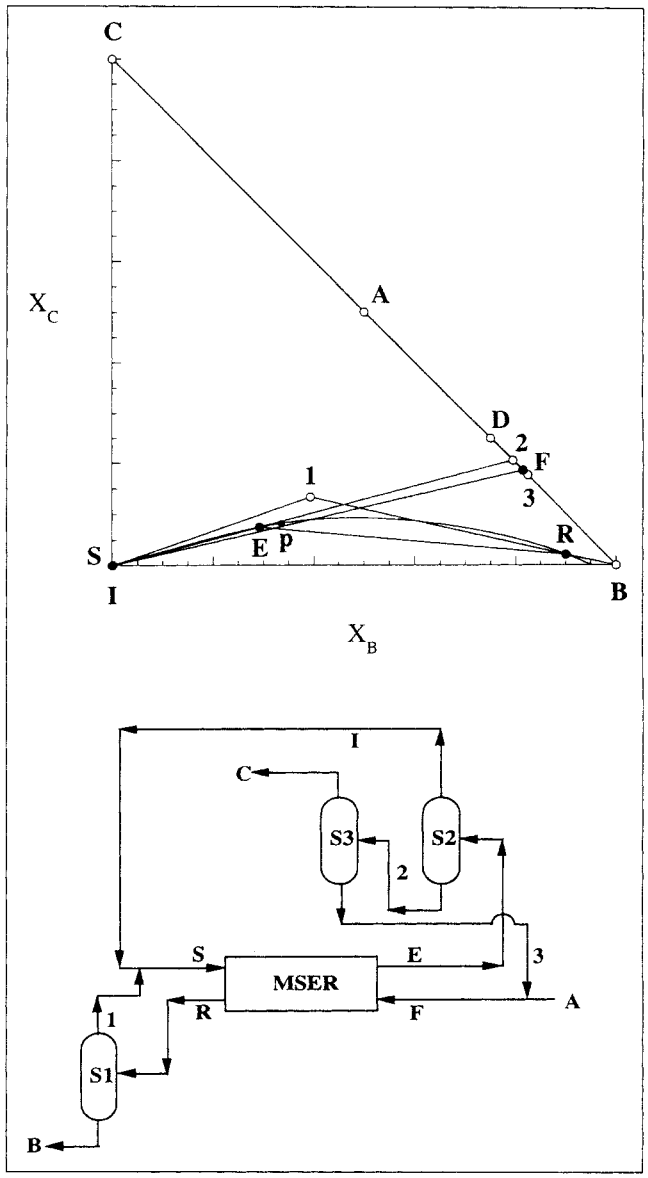

Figure 18. Improvement in selectivity: series-parallel reactions: flowsheet and phase diagram for Example V.

Example V: Series-Parallel Reactions. Consider a series-parallel reaction scheme:

$$2A \leftrightarrow B + C$$
$$A + B \leftrightarrow 2D. \tag{31}$$

The product distribution for this scheme is given by Eq. 27. Similar to the previous case, a solvent I partially miscible with B only can be successfully used to increase the product distribution. The flow sheet for this process and the corresponding phase diagram is shown in Figure 18. The transformed coordinates for this system are

$$X_B = x_B + \frac{1}{2}x_A + \frac{3}{4}x_D \tag{32}$$

$$X_C = x_C + \frac{1}{2}x_A + \frac{1}{4}x_D \tag{33}$$

$$X_I = x_I, \tag{34}$$

with A and D as reference components. The flowsheet is similar to the one used in Example III. The degrees-of-freedom analysis for the flow sheet is summarized in Table 3. For this system, the product distribution has a constant value of 0.5 for all values of the design variable $X_{B,E}$. This value is much superior to the value of 0.3862 obtainable from a single-phase process. The trade-off between MSER flows and the number of theoretical stages is also observed in this case. For the parameters chosen, however, the increase in the number of theoretical stages is not very sharp. Hence operating at a high value of $X_{B,E}$ near the plait point p may be advantageous.

Separation Processes Using Reactive Extraction

Example VI: Use of Reactive Extraction to Separate Hard-to-Separate Impurities. Consider a system comprising components A and B, where A is the desired compound and B is an impurity, which is extremely difficult to separate using traditional separation techniques. The separation task can be considerably simplified by converting B to some other compound that can be easily separated by using conventional techniques. This can be achieved by adding a solvent C that reacts with B as follows:

$$B + C \leftrightarrow D. \tag{35}$$

Both C and D can easily be separated from A. The separation can be further improved if we choose C such that the reaction product D is partially miscible with A, B, and C. Based on this idea, a flow sheet for purification of a stream containing A and B is shown in Figure 19. The figure also shows the corresponding phase diagram. The phase diagram was generated using the thermodynamic parameters for a type III four-component system listed in Table 2. The transformed mole fractions for the system are given by Eqs. 14, 15, and 16.

The feed (F), composed of A and impurity B, is combined with solvent C to form stream (1), which is fed to the reactive extractor (RE). As point 1 lies within the reactive phase envelope, the effluent comprises an extract stream (E) and a raffinate stream (R) corresponding to the end points of the reactive tie line passing through point 1. The extract stream, which is essentially a mixture of A and C with trace B and D, is sent to separator $S1$, where C is separated and sent back. D is removed from stream (2) to obtain the product stream (3), which contains much less B than the feed stream. The raffinate (R) and stream D can be treated as byproduct or waste streams. Make-up for solvent C is needed, as some C is lost through the raffinate stream.

Figure 20 shows the variation of product purity with the solvent flow rate. In this case, the product purity goes through a maximum as the solvent to feed (C/F) ratio is increased. Thus there is an upper limit on the amount of impurity that can be removed, and this limit corresponds to an optimum solvent to feed ratio. It should be noted that beyond this op-

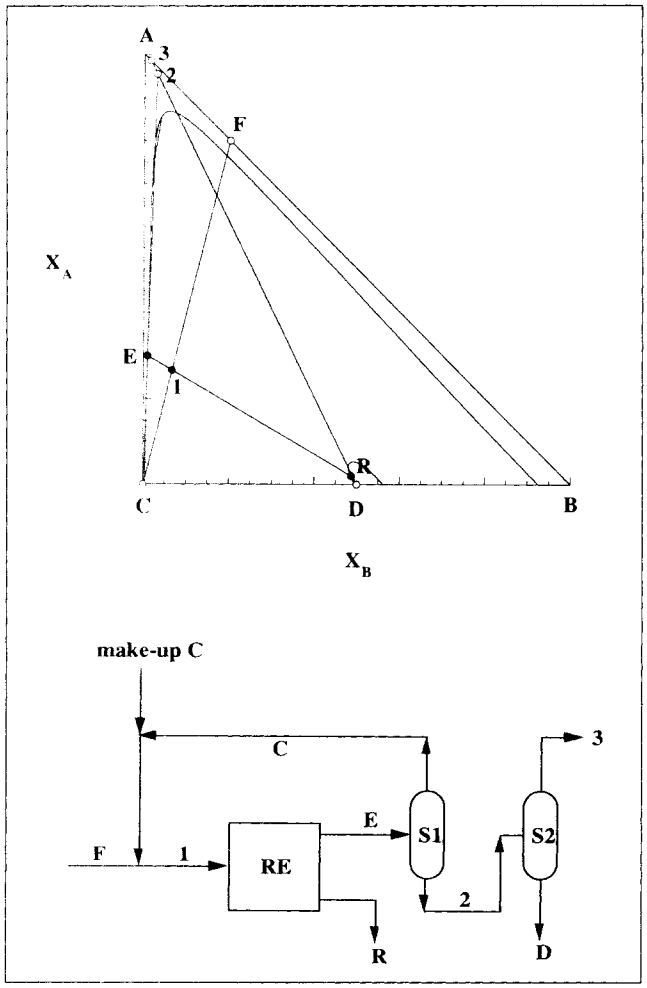

Figure 19. Reactive extraction for separation of hard-to-separate impurities: flowsheet and phase diagram for Example VI.

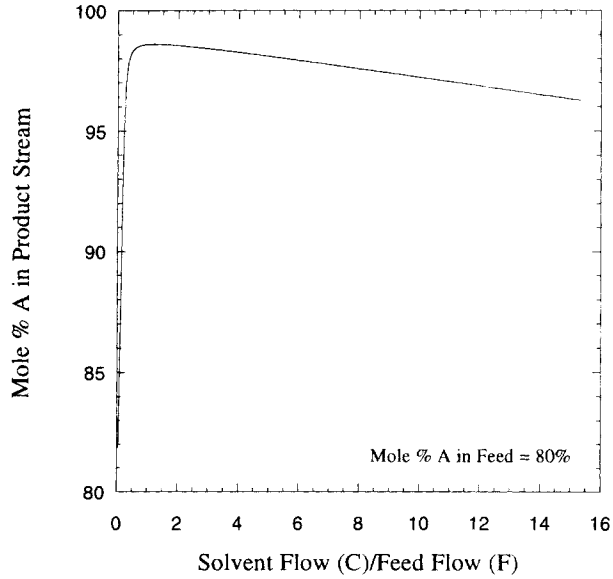

Figure 20. Product purity as a function of solvent flow rate for Example VI.

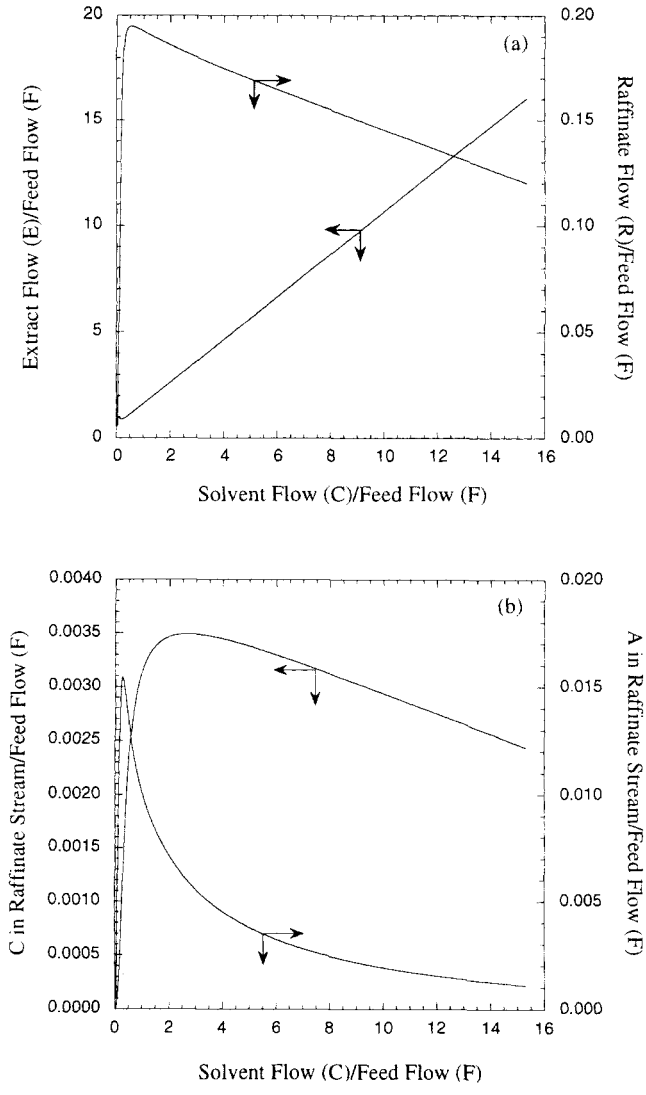

Figure 21. (a) Extract (product) and raffinate (waste) flow rates as a function of solvent flow rate for Example VI; (b) solvent (C) and reagent (A) wasted through the raffinate stream as a function of solvent flow rate for Example VI.

timum solvent to feed ratio. It should be noted that beyond this optimum solvent to feed ratio, the addition of more solvent does not give improved separation. Figure 21a shows the extract (E) and raffinate (R) flows as a function of the C/F ratio. Extract flow goes through a minimum and the raffinate flow goes through a maximum as C/F is increased. The minimum and maximum occur at the optimum C/F ratio. Figure 21b shows the amounts of C and A wasted through the raffinate stream. In general, amounts of A and C wasted decrease beyond the optimum C/F ratio. Thus, a trade-off between improved separation and increased loss of A and solvent C is observed on both sides of the optimum C/F ratio. Below the optimum, the addition of solvent improves the separation, but results in increased loss of A and C. Above the optimum, the addition of solvent decreases the loss of A and C, but does not improve the product purity.

Example VII: Reactive Extraction as an Alternative Process to Conventional Extraction. In some cases where one or more

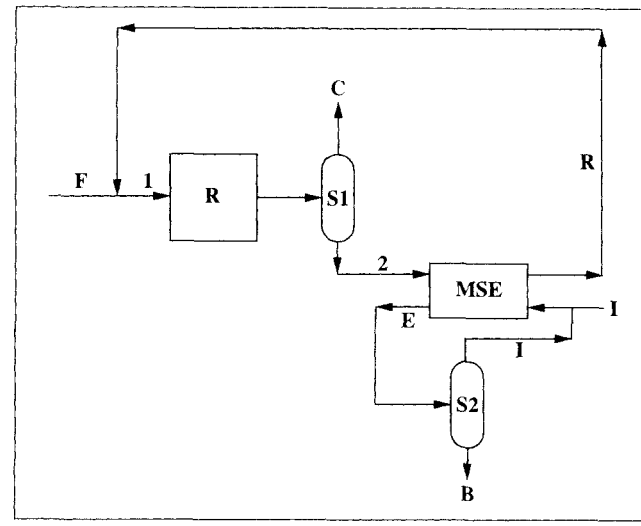

Figure 22. Conventional process flowsheet for reaction and separation by extraction.

reactants and products of a process are separated by conventional liquid–liquid extraction, reactive extraction offers an attractive process alternative by combining the reaction and extraction steps in the process. Consider the reaction

$$A \leftrightarrow B + C, \tag{36}$$

where C is the desired product. For low conversions of A, it is necessary to separate and recycle unreacted A. If A and byproduct B are close boilers, liquid–liquid extraction can be used to separate B and A. The flow sheet for such a process is shown in Figure 22. C is separated from the reactor effluent in column $S1$. Solvent I partially miscible with A is used to extract B from stream (2) in a multistage extractor (MSE). The raffinate stream (R) is mostly A and is sent back to the reactor. The extract (E) is sent to the solvent recovery column $S2$, where solvent I is separated and recycled to the MSE.

We can combine the reaction and extraction operations by using an MSER cascade, which employs a solvent that is partially miscible with B. The flow sheet for such a process is shown in Figure 23. The phase diagram for the system is also shown in the figure. MSER cascade is operated within the two-phase region such that the raffinate stream (R) is composed mostly of B. Solvent I is separated from the extract stream (E) in separator $S1$ and is fed back to the MSER. Product C is removed from stream (1) in separator $S2$, and stream (2) is mixed with fresh reactant A to form the feed stream to the MSER. As shown earlier in Example III, with a proper choice of solvent I, this flow sheet can also be effectively used to improve the per-pass yield of product C.

Conclusions

This article examines the use of reactive two-phase liquid–liquid systems for performing simultaneous reaction and separation. Such systems can be obtained either by deliberate addition of an immiscible liquid phase or can occur due to the formation of a byproduct that is partially miscible with

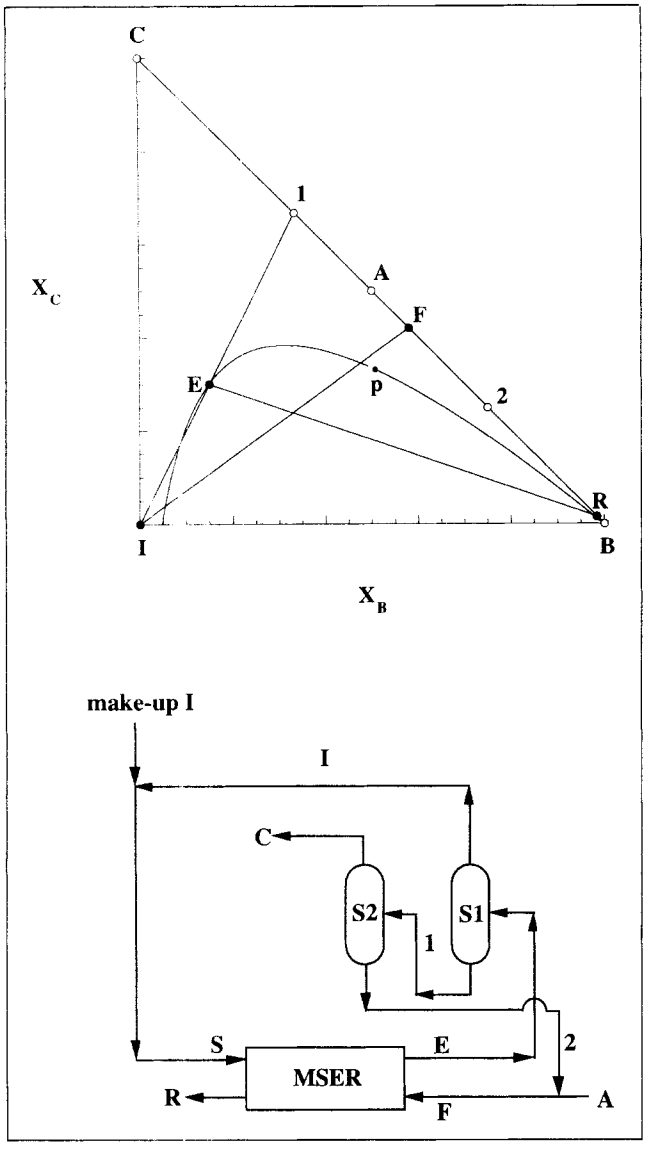

Figure 23. Reactive extraction as an alternative to conventional process; flowsheet and phase diagram.

the reactants, such as water in an organic reaction. The objective of this article is to provide a more systematic approach based on equilibrium thermodynamic analysis for synthesizing process flow sheets that can more fully exploit the potential benefits of these systems.

An important component of this procedure is the calculation and representation of multicomponent reactive liquid–liquid phase diagrams. It is illustrated with several examples of three- and four-component systems. The phase diagrams are plotted in mole-fraction coordinates or transformed mole-fraction coordinates. The latter is one of the methods for projecting high dimensional phase diagrams onto a lower dimensional space; see Dye and Ng (1995), and Berry and Ng (1996) for other related techniques. Use of transformed mole fractions eliminates the restriction on visualization of phase behavior for systems with more than three components. A point on the transformed coordinate phase diagram represents a unique composition that satisfies both phase and reaction equilibrium. However, for process synthesis we have to represent compositions that do not satisfy reaction equilibrium and material balances that do not involve reactions on the transformed phase diagram. As demonstrated in Appendix C, since the transformed lever rule still holds for both reactive and nonreactive liquid–liquid systems, we can still use a transformed coordinate phase diagram for synthesizing process flow sheets provided care is exercised in ensuring the feasibility of the nonreactive moves on the phase diagram.

Potential improvements in yield, selectivity, and separations of extractive reaction processes over single-phase processes are demonstrated with examples. Phase diagrams for these processes are generated based on realistic thermodynamic data in the literature. The corresponding process flow sheets are also provided. We have identified the design variables using degrees-of-freedom analysis. For some examples the dependence of the objective function on the design variables is quantified and process trade-offs are evaluated. The various features of the phase diagram necessary to achieve the objectives are also highlighted. For example, improvement in yield or selectivity can be achieved by using a solvent that is miscible with the desired product relative to other components (Example I) or immiscible with the desired product (Examples III, IV and V). For systems that are restricted to low per-pass yield due to the presence of an immiscibility gap, a solvent can be used to provide an additional degree of freedom. This can be utilized to cross the gap and obtain substantially higher yield (Example II). If the liquid–liquid region has more than one degree of freedom, the use of a cascade of extractive reactors provides a means for enhancing reactor performance (Examples II, IV, and V). With suitable solvents, extractive reaction can be used for separating hard-to-separate impurities (Example VI) and as an alternative to conventional extraction (Example VII).

In addition to providing insights for process development, this procedure can also be used to help in screening solvents with desired properties. In general, data for liquid–liquid phase separation in multicomponent mixtures are not readily available. Our analysis can be used to determine what data are needed and the region of composition space where the experimental efforts should be focused. The performance of extractive reaction processes discussed in this article is also often limited by reaction kinetics and mass transfer. Efforts to include effects of reaction kinetics and mass-transfer limitations are currently underway.

Acknowledgment

Financial support from the National Environmental Technology Institute is gratefully acknowledged.

Literature Cited

Anderson, W. K., and T. Veysoglu, "A Simple Procedure for the Epoxidation of Acid Sensitive Olefinic Compound with m-Chlorperbenzoic Acid in an Alkaline Biphasic Solvent System," *J. Org. Chem.*, **38**, 2267 (1973).

Berry, D. A., and K. M. Ng, "Separation of Quaternary Conjugate Salt Systems by Fractional Crystallization," *AIChE J.*, **42**, 2162 (1996).

Berry, D. A., and K. M. Ng, "Synthesis of Reactive Crystallization Processes," *AIChE J.*, **43**, 1737 (1997).

Chapman, T. W., "Extraction—Metals Processing," *Handbook of Separation Process Technology*, R. W. Rousseau, ed., Wiley, New York (1987).
Coca, J., G. Adrio, C. Y. Jeng, and S. H. Langer, "Gas and Liquid Chromatographic Reactors," *Preparative and Production Scale Chromatography*, G. Ganestos and P. E. Barker, eds., Dekker, New York (1993).
DeGarmo, J. L., V. N. Parulekar, and V. Pinjala, "Consider Reactive Distillation," *Chem. Eng. Prog.*, **3**, 43 (1992).
Doherty, M. F., and G. Buzad, "Reactive Distillation by Design," *Trans. Inst. Chem. Eng.*, **70**, 448 (1992).
Dye, S. R., and K. M. Ng, "Bypassing Eutectics with Extractive Crystallization: Design Alternatives and Tradeoffs," *AIChE J.*, **41**, 1456 (1995).
Harold, M. P., J. J. Ostermaier, D. W. Drew, J. J. Lerou, and D. Luss, "The Continuously-Stirred Decanting Reactor: Steady State and Dynamic Features," *Chem. Eng. Sci.*, **51**, 1777 (1996).
King, M. L., A. L. Forman, C. Orella, and S. H. Pines, "Extractive Hydrolysis for Pharmaceuticals," *Chem. Eng. Prog.*, **5**, 36 (1985).
Kuntz, E. G., "Homogeneous Catalysis in Water," *CHEMTECH*, **9**, 570 (1987).
Mersmann, A., and M. Kind, "Chemical Engineering Aspects of Precipitation from Solution," *Chem. Eng. Tech.*, **11**, 264 (1988).
Pahari, P. K., and M. M. Sharma, "Recovery of Morpholine via Reactive Extraction," *Ind. Eng. Chem. Res.*, **30**, 2015 (1991).
Prausnitz, J. M., T. F. Anderson, E. A. Grens, C. A. Eckert, R. Hsieh, and J. P. O'Connell, *Computer Calculations for Multicomponent Vapor-Liquid and Liquid-Liquid Equilibria*, Prentice Hall, Englewood Cliffs, NJ (1980).
Sharma, M. M., "Multiphase Reactions in the Manufacture of Fine Chemicals," *Chem. Eng. Sci.*, **43**, 1749 (1988).
Sorenson, J. M., and W. Arlt, "Liquid-Liquid Equilibrium Data Collection," *DECHEMA Chem. Data Ser.*, Vol. 5, Parts 2 and 3, DECHEMA, Frankfurt (1979).
Tonkovich, A. L. Y., and R. W. Carr, "Modeling of the Simulated Countercurrent Moving-Bed Chromatographic Reactor Used for the Oxidative Coupling of Methane," *Chem. Eng. Sci.*, **49**, 4657 (1994).
Tsotsis, T. T., A. M. Champagnie, R. G. Minet, and P. K. T. Liu, "Catalytic Membrane Reactors," *Computer Aided Design of Catalysts*, R. E. Becker and C. Pereira, eds., Dekker, New York (1993).
Ung, S., and M. F. Doherty, "Vapor-Liquid Phase Equilibrium in Systems with Multiple Chemical Reactions," *Chem. Eng. Sci.*, **50**, 23 (1995a).
Ung, S., and M. F. Doherty, "Synthesis of Reactive Distillation Systems with Multiple Equilibrium Chemical Reactions," *Ind. Eng. Chem. Res.*, **34**, 2555 (1995b).
Wang, S., Z. Wang, Z. Xu, Y. Wang, S. Wu, and X. Huang, "Study on the Hofmann Reagents in a Two Phase System," *Chem. Abstr.*, **101**, 90361 (1984).

Appendix A: Definition and Properties of Transformed Mole-Fraction Coordinates

Definition

Consider a system of r independent reactions among c reacting components. The chemical reaction can be represented as

$$\upsilon_{1,m}A_1 + \upsilon_{2,m}A_2 + \cdots + \upsilon_{c,m}A_c = 0 \qquad m = 1,2, \ldots, r, \tag{A1}$$

where A_i are the reacting species and $\upsilon_{i,m}$ is the stoichiometric coefficient of component i in reaction m. Using vector-matrix formalism, we define:

$$\upsilon_i^T = (\upsilon_{i,1}, \upsilon_{i,2}, \ldots, \upsilon_{i,r}) \tag{A2}$$

$$\upsilon_{\mathrm{TOT}}^T = (\upsilon_{\mathrm{TOT},1}, \upsilon_{\mathrm{TOT},2}, \ldots, \upsilon_{\mathrm{TOT},r}), \tag{A3}$$

where υ_i^T is the row vector of stoichiometric coefficients of component i in each reaction and $\upsilon_{\mathrm{TOT}}^T$ is the row vector of the sum of the stoichiometric coefficients for each reaction. We choose r reference components and define:

$$\boldsymbol{x}_{\mathrm{Ref}} = (x_{(c-r+1)}, x_{(c-r+2)}, \ldots, x_c)^T \tag{A4}$$

$$\boldsymbol{V} = \begin{pmatrix} \upsilon_{(c-r+1),1} & \cdots & \upsilon_{(c-r+1),r} \\ \cdots & \upsilon_{i,r} & \cdots \\ \upsilon_{c,1} & \cdots & \upsilon_{c,r} \end{pmatrix}, \tag{A5}$$

where $\boldsymbol{x}_{\mathrm{Ref}}$ is the column vector composed of the mole fractions of the r reference components and $\boldsymbol{V}$ is the square matrix of stoichiometric coefficients for the r reference components in the r reactions. Reference components are chosen such that the matrix $\boldsymbol{V}$ is invertible. Such a choice is always possible (Ung and Doherty, 1995a).

The transformed mole-fraction coordinates can now be defined as

$$X_i = \frac{x_i - \upsilon_i^T \boldsymbol{V}^{-1}\boldsymbol{x}_{\mathrm{Ref}}}{1 - \upsilon_{\mathrm{TOT}}^T \boldsymbol{V}^{-1}\boldsymbol{x}_{\mathrm{Ref}}} \qquad i = 1,2, \ldots, c-r. \tag{A6}$$

Properties

1. The transformed mole fractions sum to unity

$$\sum_{i=1}^{c-r} X_i = 1. \tag{A7}$$

2. Transformed mole fractions are reaction invariant:

$$X_i(0) = X_i(\boldsymbol{\xi}) \qquad \forall \boldsymbol{\xi} \qquad i = 1,2, \ldots, c-r, \tag{A8}$$

where $\boldsymbol{\xi}$ is the column vector of the r dimensionless extents of reaction

$$\boldsymbol{\xi} = (\xi_1, \xi_2, \ldots, \xi_r)^T. \tag{A9}$$

This implies that the transformed coordinates describe the system as if no reactions were occurring at all. This eliminates the problem of drawing stoichiometric lines for multiple reactions with complex chemistries.

Appendix B: Method for Calculating Phase and Chemical Equilibrium for Multicomponent Liquid–Liquid Mixtures with Multiple Chemical Reactions

Consider a system of c components with r independent chemical reactions. There are c liquid–liquid phase-equilibrium equations simultaneously satisfied with r thermodynamic reaction equilibrium equations:

$$(\gamma_i x_i)^{\mathrm{I}} = (\gamma_i x_i)^{\mathrm{II}} \qquad i = 1,2, \ldots, c \tag{B1}$$

$$K_m = \prod_{i=1}^{c} \left[(\gamma_i x_i)^{\mathrm{I}}\right]^{\upsilon_{i,m}} \qquad m = 1, 2, \ldots, r. \tag{B2}$$

Superscripts I and II indicate liquid phases I and II, respectively. Subscript *eq.* which indicates reaction equilibrium, is dropped for convenience.

In addition, we have

$$\sum_{i=1}^{c} x_i^{\mathrm{I}} = 1 \tag{B3}$$

$$\sum_{i=1}^{c} x_i^{\mathrm{II}} = 1. \tag{B4}$$

If we choose r reference components and derive the $(c-r)$ transformed mole fractions for each phase, we can write

$$X_i^I = \frac{x_i^I - v_i^T V^{-1} x_{\mathrm{Ref}}^{\mathrm{I}}}{1 - v_{\mathrm{TOT}}^T V^{-1} x_{\mathrm{Ref}}^{\mathrm{I}}} \qquad i = 1,2, \ldots, c-r-1 \tag{B5}$$

$$X_i^{\mathrm{II}} = \frac{x_i^{\mathrm{II}} - v_i^T V^{-1} x_{\mathrm{Ref}}^{\mathrm{II}}}{1 - v_{\mathrm{TOT}}^T V^{-1} x_{\mathrm{Ref}}^{\mathrm{II}}} \qquad i = 1,2, \ldots, c-r-1 \tag{B6}$$

$$\sum_{i=1}^{c-r} X_i^{\mathrm{I}} = 1 \tag{B7}$$

$$\sum_{i=1}^{c-r} X_i^{\mathrm{II}} = 1. \tag{B8}$$

If we denote the feed mole fractions and transformed mole fractions by x_i^F and X_i^F, respectively, we have

$$\sum_{i=1}^{c} x_i^F = 1 \tag{B9}$$

$$X_i^F = \frac{x_i^F - v_i^T V^{-1} x_{\mathrm{Ref}}^F}{1 - v_{\mathrm{TOT}}^T V^{-1} x_{\mathrm{Ref}}^F} \qquad i = 1,2, \ldots, c-r-1 \tag{B10}$$

$$\sum_{i=1}^{c-r} X_i^F = 1. \tag{B11}$$

The lever rule is obeyed in the transformed coordinates as shown in Appendix C. Hence we can also write:

$$\phi X_i^{\mathrm{I}} + (1-\phi) X_i^{\mathrm{II}} = X_i^F \qquad i = 1,2, \ldots, c-r-1, \tag{B12}$$

where $0 \le \phi \le 1$ and ϕ is the fraction of phase I in the mixture at phase and reaction equilibrium.

Therefore, the total number of equations is $5c-3r+2$. These equations contain the following $6c-3r+3$ variables, x^{I}, x^{II}, x^F, X^{I}, X^{II}, X^F, ϕ, T, and P. Hence at fixed temperature (T) and pressure (P), we have $(c-1)$ degrees of freedom for this set of equations. The algorithm for solving this set is described below. This algorithm is not claimed to be the most efficient method.

Algorithm

(1) Fix T and P.

Fix $(c-1)$ degrees of freedom as follows:

Fix $c-r-1$ transformed feed mole fractions X_i^F, $i = 1, 2, \ldots, c-r-1$.

Fix r feed mole fractions of the reference components x_i^F, $i = c-r+1, \ldots, c$ (i.e., x_{Ref}^F).

(2) Set all liquid phase activity coefficients to unity.

$\gamma_i^{\mathrm{I}} = \gamma_i^{\mathrm{II}} = 1 \qquad i = 1, 2, \ldots, c.$

(3) Calculate the last transformed feed mole fraction, X_{c-r}^F, using Eq. B11.

Calculate the feed mole fractions $x_i^F, i = 1, 2, \ldots, c-r$, using Eqs. B9, B10, and x_{Ref}^F.

(4) Pick an initial guess for the following $(c+r)$ variables: x_i^{I}, $i = 1,2, \ldots, c-1$; x_i^{II}, $i = c-r+1, \ldots, c$ (i.e., $x_{\mathrm{Ref}}^{\mathrm{II}}$); and ϕ.

(5) Calculate x_c^{I} using Eq. B3.

Calculate X_i^{I}, $i = 1,2, \ldots, c-r$ using Eqs. B5 and B7.

Calculate X_i^{II}, $i = 1,2, \ldots, c-r$ using Eqs. B8 and B12.

Calculate $x_i^{\mathrm{II}}, i = 1,2, \ldots, c-r$ using Eqs. B4 and B6 and $x_{\mathrm{Ref}}^{\mathrm{II}}$.

(6) Calculate the liquid-phase activity coefficients for both phases. We have used the UNIQUAC equation for this step. Any thermodynamically consistent model can be used in its place.

(7) Calculate the following functions:

$F(m) = \prod_{i=1}^{c} [(\gamma_i x_i)^{\mathrm{I}}]^{v_{i,m}} - K_m(T) \qquad m = 1,2, \ldots, r$

$F(n) = (\gamma_{n-r} x_{n-r})^{\mathrm{I}} - (\gamma_{n-r} x_{n-r})^{\mathrm{II}} \qquad n = r+1, r+2, \ldots, c+r$

which determine F, a column vector of residuals of dimension $(c+r)$.

(8) If $|F| > \epsilon$ (a vector of set tolerances), then go to step (4) and simultaneously update the values for the guesses. For this step, we use Newton's method with a finite difference approximation to the Jacobian. Otherwise STOP. The current values for x^{I}, x^{II}, X^{I}, X^{II}, and ϕ represent the solution to the problem at the given T and P. Care is taken to ensure that the values of x^{I}, x^{II}, and ϕ lie between zero and one.

Appendix C: Representation of Material Balances with or without Reactions in Transformed Coordinates

Material balance with reactions

Consider a system of c components with r independent reactions. Let the feed flow rate to the system be F and the flow rates of the two product streams be E and R. We can write the material balance equations as

$$Fz_i = Ex_i + Ry_i - v_i^T \epsilon \qquad i = 1, 2, \ldots, c, \tag{C1}$$

where z_i, x_i, and y_i are mole fractions of component i in the feed and the two product streams, respectively, and $\epsilon = (\epsilon_1, \epsilon_2, \ldots, \epsilon_r)^T$ is the column vector of r molar extents of reaction. By choosing r reference components, we can split Eq. C1 as

$$Fz_{\mathrm{Ref}} = Ex_{\mathrm{Ref}} + Ry_{\mathrm{Ref}} - V\epsilon \tag{C2}$$

$$Fz_i = Ex_i + Ry_i - v_i^T \epsilon \qquad i = 1,2, \ldots, c-r-1 \tag{C3}$$

$$F = E + R - v_{\mathrm{TOT}}^T \epsilon, \tag{C4}$$

where z_{Ref}, x_{Ref}, and y_{Ref} are column vectors of reference component mole fractions for the feed and the two product streams, respectively.

Eliminating ϵ from Eqs. C3 and C4 by using Eq. C2 and rearranging, we get

$$F(z_i - v_i^T V^{-1} z_{\text{Ref}}) = E(x_i - v_i^T V^{-1} x_{\text{Ref}}) + R(y_i - v_i^T V^{-1} y_{\text{Ref}})$$
$$i = 1, 2, \ldots, c - r - 1 \quad \text{(C5)}$$

$$F(1 - v_{\text{TOT}}^T V^{-1} z_{\text{Ref}}) = E(1 - v_{\text{TOT}}^T V^{-1} x_{\text{Ref}}) + R(1 - v_{\text{TOT}}^T V^{-1} y_{\text{Ref}}). \quad \text{(C6)}$$

We now define the transformed flow rates as

$$\hat{F} = F(1 - v_{\text{TOT}}^T V^{-1} z_{\text{Ref}}) \quad \text{(C7)}$$

$$\hat{E} = E(1 - v_{\text{TOT}}^T V^{-1} x_{\text{Ref}}) \quad \text{(C8)}$$

$$\hat{R} = R(1 - v_{\text{TOT}}^T V^{-1} y_{\text{Ref}}) \quad \text{(C9)}$$

and rewrite Eqs. C5 and C6 as

$$\hat{F} Z_i = \hat{E} X_i + \hat{R} Y_i \qquad i = 1, 2, \ldots, c - r - 1 \quad \text{(C10)}$$

$$\hat{F} = \hat{E} + \hat{R}. \quad \text{(C11)}$$

Equations C10 and C11 completely represent the material balance for this system. Using Eqs. C10 and C11, the ratio of the transformed flow rates of the two product phases can be written as

$$\frac{\hat{E}}{\hat{R}} = \frac{Y_i - Z_i}{Z_i - X_i} \qquad i = 1, 2, \ldots, c - r. \quad \text{(C12)}$$

Equation C12 is the lever rule in terms of transformed coordinates. It has the same functional form as the lever rule in terms of mole fractions for nonreactive mixtures.

Material balance without reactions

For the same system of c components, the material-balance equations in the absence of any reactions can be written as

$$F z_i = E x_i + R y_i \qquad i = 1, 2, \ldots, c. \quad \text{(C13)}$$

By choosing the same r reference components, we can split these equations as

$$F z_{\text{Ref}} = E x_{\text{Ref}} + R y_{\text{Ref}} \quad \text{(C14)}$$

$$F z_i = E x_i + R y_i \qquad i = 1, 2, \ldots, c - r - 1 \quad \text{(C15)}$$

$$F = E + R. \quad \text{(C16)}$$

From the definition of the transformed coordinates, we have

$$z_i = Z_i(1 - v_{\text{TOT}}^T V^{-1} z_{\text{Ref}}) + v_i^T V^{-1} z_{\text{Ref}} \quad \text{(C17)}$$

$$x_i = X_i(1 - v_{\text{TOT}}^T V^{-1} x_{\text{Ref}}) + v_i^T V^{-1} x_{\text{Ref}} \quad \text{(C18)}$$

$$y_i = Y_i(1 - v_{\text{TOT}}^T V^{-1} y_{\text{Ref}}) + v_i^T V^{-1} y_{\text{Ref}}. \quad \text{(C19)}$$

Using these equations and the definitions of the transformed flow rates, Eq. C15 can be rewritten as

$$\hat{F} Z_i = \hat{E} X_i + \hat{R} Y_i + v_i^T V^{-1}(E x_{\text{Ref}} + R y_{\text{Ref}} - F z_{\text{Ref}})$$
$$i = 1, 2, \ldots, c - r - 1. \quad \text{(C20)}$$

Equation C16 can also be rewritten as

$$\hat{F} = \hat{E} + \hat{R} + v_{\text{TOT}}^T V^{-1}(E x_{\text{Ref}} + R y_{\text{Ref}} - F z_{\text{Ref}}). \quad \text{(C21)}$$

The term inside the parentheses in Eqs. C20 and C21 is zero (Eq. C14). Thus, we get

$$\hat{F} Z_i = \hat{E} X_i + \hat{R} Y_i \qquad i = 1, 2, \ldots, c - r - 1 \quad \text{(C22)}$$

$$\hat{F} = \hat{E} + \hat{R}. \quad \text{(C23)}$$

These equations are the same as Eqs. C10 and C11. Thus, even in the absence of a reaction the system obeys the lever rule in terms of transformed coordinates (Eq. C12). However, in this case the $(c - r)$ Eqs. C22 and C23 do not describe the material balance completely. Additional r equations given by Eq. C14 complete the description. This is due to the fact that the transformed coordinates correspond, in principle, only to compositions that satisfy reaction-equilibrium equations.

These additional equations limit the attainable regions for product compositions that can be obtained from a given feed composition. This can be better explained with the aid of Figure C1. Consider a single-phase system comprising four components, A, B, C, and D, with the reaction described by Eq. 13. With D as the reference component, the transformed mole fractions are given by Eqs. 14, 15, and 16. Now, in the absence of the reaction, consider two feed streams $F1$ and

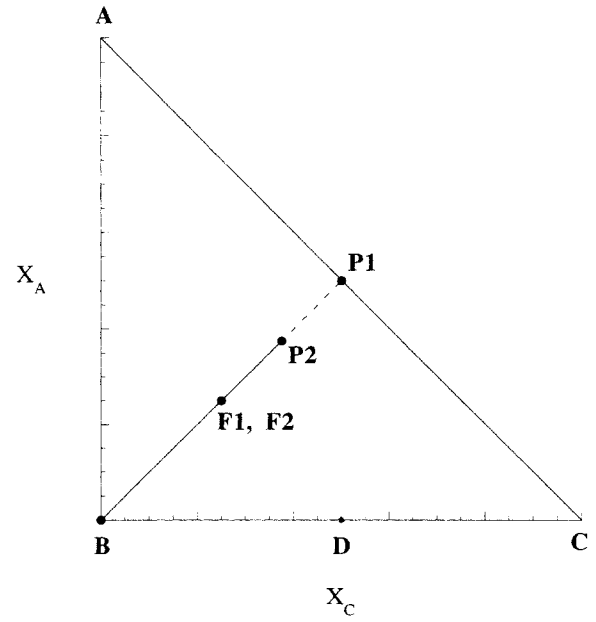

Figure C1. Material balances with or without reactions in transformed coordinates.

$F2$ with compositions $\{x_A = 0.25,\ x_B = 0.5,\ x_C = 0.25,\ x_D = 0.0\}$, and $\{x_A = 0.3,\ x_B = 0.4,\ x_C = 0.1,\ x_D = 0.2\}$, respectively. The transformed mole fractions for both streams are $\{X_A = 0.25,\ X_B = 0.5,\ X_C = 0.25\}$. By completely separating B from stream $F1$, we can get a product stream corresponding to point $P1$ on the nonreactive $A-C$ edge. However, this is not possible for stream $F2$. We can never reach the nonreactive $A-C$ edge of the phase diagram by removing B from $F2$, as $F2$ contains component D. Complete removal of B can take us only as far as point P_2. Thus, although streams $F1$ and $F2$ correspond to the same point on the transformed coordinate phase diagram, the product composition attainable by separation of stream $F2$ is limited by Eq. C14.

Often for the synthesis of process flow sheets and screening of alternatives, we plot the material balance lines on the transformed coordinate phase diagrams without actually calculating the mole fractions of each stream. By plotting material balance lines for separations without reaction, we represent a $(c-1)$ dimensional system on a $(c-r-1)$ dimensional phase diagram. Hence, care must be taken to make sure that the product compositions are attainable by checking whether the r equations given by Eq. C14 are satisfied.

Manuscript received Oct. 9, 1997, and revision received Feb. 17, 1998.